The barley leaf rust resistance gene Rph3 encodes a putative executor protein

Hoan Dinh
Plant Protection Research Institute https://orcid.org/0000-0001-6442-0416
Davinder Singh
University of Sydney
Diana Cruz
The Sainsbury Laboratory
Goetz Hensel
Leibniz Institute of Plant Genetics and Crop Plant Research (IPK)
Martin Mascher
Leibniz Institute of Plant Genetics and Crop Plant Research (IPK) Gatersleben https://orcid.org/0000-0001-6373-6013
Nils Stein
Leibniz Institute of Plant Genetics and Crop Plant Research https://orcid.org/0000-0003-3011-8731
Dragan Perovic
Julius Kühn-Institut - Federal Research Centre for Cultivated Plants
Michael Ayliffe
CSIRO Agriculture
Matthew Moscou
The Sainsbury Laboratory https://orcid.org/0000-0003-2098-6818
Robert Park
University of Sydney https://orcid.org/0000-0002-9145-5371
Mohammad pourkheirandish (mohammad.p@unimelb.edu.au)
The University of Melbourne https://orcid.org/0000-0003-4337-3600

Article

Keywords: host resistance, plant diseases, executor genes

Posted Date: July 30th, 2021

DOI: https://doi.org/10.21203/rs.3.rs-729002/v1

The barley leaf rust resistance gene *Rph3* encodes a putative executor protein

Hoan X. Dinh[a], Davinder Singh[a], Diana Gomez de la Cruz[c], Goetz Hensel[d,e], Martin Mascher[d,f], Nils Stein[d,g], Dragan Perovic[h], Michael Ayliffe[i], Matthew J. Moscou[c], Robert F. Park[a1], Mohammad Pourkheirandish[b1]

[a]The University of Sydney, Faculty of Science, Plant Breeding Institute, Cobbitty, NSW 2570, Australia

[b]The University of Melbourne, Faculty of Veterinary and Agriculture, Parkville 3010, Australia

[c]The Sainsbury Laboratory, University of East Anglia, Norwich Research Park, Norwich NR4 7UK, UK

[d]Leibniz Institute of Plant Genetics and Crop Plant Research (IPK), Corrensstr. 3, 06466 Seeland, Germany

[e]Centre of the Region Haná for Biotechnological and Agricultural Research, Czech Advanced Technology and Research Institute, Palacký University Olomouc, 78371 Olomouc, Czech Republic

[f]German Centre for Integrative Biodiversity Research (iDiv) Halle-Jena-Leipzig, Leipzig, Germany

[g]Center of integrated Breeding Research (CiBreed), Department of Crop Sciences, Georg-August-University, Von Siebold Str. 8, 37075 Göttingen, Germany

[h]Julius Kühn-Institut, Institute for Resistance Research and Stress Tolerance, Erwin-Baur-Strasse 27, 06484 Quedlinburg, Germany

[i]Commonwealth Scientific and Industrial Research Organisation, Black Mountain ACT 2601, Australia

[1]To whom correspondence may be addressed. Email: mohammad.p@unimelb.edu.au, robert.park@sydney.edu.au

The authors declare no conflict of interest.

Abstract

Host resistance is considered the most effective means to control plant diseases; however, individually deployed resistance genes are often rapidly overcome by pathogen adaptation. Combining multiple effective resistance genes is the optimal approach to durable resistance, but the lack of functional markers for resistance genes has hampered implementation. Leaf rust, caused by *Puccinia hordei*, is an economically significant disease of barley, but only a few major Resistance genes to *P. hordei* (*Rph*) have been cloned. In this study, gene *Rph3* was isolated by positional cloning and confirmed by mutational analysis and transgenic complementation. The *Rph3* gene, which originated from wild barley and was first introgressed into cultivated Egyptian germplasm, encodes a unique transmembrane resistance protein that differs from all known plant disease resistance proteins at the amino acid sequence level. Genetic profiles of diverse accessions indicated limited genetic diversity in *Rph3* in domesticated germplasm, and higher diversity in wild barley from the Eastern Mediterranean region. Expression profiling using *P. hordei* isolates with contrasting pathogenicity for the *Rph3* host locus showed that the *Rph3* gene was expressed only in interactions with *Rph3*-avirulent isolates, a phenomenon also observed for transcription activator-like effector-dependent genes known as executors conferring resistance to *Xanthomonas* spp. Like the known transmembrane executors such as *Bs3* and *Xa7* heterologous expression of *Rph3* in *N. benthamiana* induced a cell death response. Given that *Rph3* shares several features with executor genes, it seems likely that *P. hordei* contains effectors similar to the transcription activator-like effectors that target host executor genes. The isolation of *Rph3* highlights convergent evolutionary processes in diverse plant-pathogen interaction systems, where similar defence mechanisms evolved independently in monocots and dicots and provide evidence for executor genes in the Triticeae tribe.

Introduction

Global food production is reduced by at least 10% by a wide range of microbial pathogens of plants [1,2]. Deployment of resistance genes has long been considered the most cost-effective and environmentally friendly method to protect crops against pathogens [1,3,4]. However, the effectiveness of resistance genes is often limited to a few years as pathogens evolve rapidly to acquire virulence that erodes or defeats genetic protection [5]. The constant conflict between host plants and their pathogens shapes genetic diversity in both organisms. Rust pathogens are obligate biotrophic fungi that can grow and reproduce only on living host tissues [6]. They cause devastating losses in agricultural production worldwide [5,7], and remain a major threat to cereal production because of the ongoing evolution of virulence that overcomes genetic resistance and can lead to complete crop loss in extreme epidemic situations [8].

To date, 106 loci conferring resistance to the leaf rust pathogens of wheat (*Puccinia triticina*) and barley (*P. hordei*) have been formally catalogued [5]. Resistance alleles for only ten of these genes have been cloned with six encoding nucleotide-binding, leucine-rich repeat (NLR) immune receptors [9-15]. The three remaining genes encode an ATP-binding cassette (ABC) transporter [16], a hexose transporter [17], and a lectin receptor kinase [18]. At least 28 resistance loci have been catalogued as *Reaction to Puccinia hordei* or *Rph* loci (*Rph1* to *Rph27*) [7,19-21], among which a few, including *Rph3* [7], have been deployed in commercial barley cultivars. Only three (*viz*. *Rph1, Rph15,* and *Rph22*) of these genes have been cloned, in part due to the difficulties imposed by the large and repetitive barley genome, highlighting a knowledge gap in this area. The resistance phenotypes conferred by *Rph* genes range from complete immunity (no visual symptoms) to small uredinia with restricted growth. The *Rph3* locus, previously known as *Pa3*, was first discovered in barley landrace 'Estate' using classical genetics [22]. The locus was mapped on the long arm of chromosome 7H and linked to the morphological X_a locus, the mutant allele confers a Xantha seedling phenotype [23]. Pathotypes with virulence for *Rph3* were detected throughout Europe [24], New Zealand [25], South America, and the Middle East [26]. In Australia, virulence for *Rph3* was first detected in 2009 and has since become common in all barley growing areas ([27] *SI Appendix*, Table S1). While *Rph3* provides high levels of resistance to avirulent pathotypes, virulence has occurred independently several times. Nonetheless, it remains a valuable source of resistance that can be deployed in combination with other widely effective resistance genes in regions where virulence is infrequent or absent.

The plant immune system encompasses two layers of defence comprising pathogen associated molecular pattern-triggered immunity (PTI) and effector-triggered immunity (ETI) [5]. In the current model of the plant immune system, PTI is mediated by receptor-like proteins (RLPs) or receptor-like kinases (RLKs) that are localized on the cell membrane [28,29], and ETI is mediated by intracellular sensors such as NLRs that are located in the cytoplasm [30]. In the process of invading mesophyll cells, rust pathogens secrete effector proteins to promote colonization [31]. Some of these effectors are recognized by corresponding receptors encoded by the host. Most of the known intracellular receptors are NLR proteins [32,33] that recognize pathogen effectors by direct [9,10,12,34] or indirect interaction [35-37]. Pathogen recognition is followed by signal transduction through various cascades to activate the immune system and trigger defence response. The vast majority of cloned race-specific resistance

genes (“R genes”) encode NLRs, and the detailed mechanism of resistance associated with them contains unknown factors [38]. A significant knowledge gap concerns other molecular partners involved in the process of signalling by NLR proteins. Discovering these signalling components could improve the breeding and engineering of crops for disease resistance. Also, a more comprehensive understanding of the repertoire of plant resistance genes will enhance knowledge of plant-pathogen defence biology and facilitate diversification of strategies for disease control.

In this study, we isolated the leaf rust resistance gene *Rph3* in barley by positional cloning and mutagenesis. *Rph3* encodes a putative transmembrane protein with no homology at mino acid level to any plant disease resistance gene isolated to date. We investigated the mechanism underlying this resistance gene and show that *Rph3* is expressed only after a challenge by rust isolates containing the corresponding *AvrRph3* gene. The *Rph3* gene was sufficient to provide resistance to *P. hordei*, and expression of the *Rph3* gene causes cell death in barley and *Nicotiana benthamiana*. These results provide evidence for the existence of ‘executor’ genes in the Triticeae.

Results

***Rph3* is an incompletely dominant gene that confers resistance to *P. hordei*.** Barley line BW746 (Bowman*11/Estate) is near-isogenic to cultivar (cv.) Bowman and carries the *Rph3.c* allele from the landrace Estate. Having ten backcrosses to cv. Bowman, this line comprises more than 99% of the recipient cultivar genome. Inoculation with *P. hordei* pathotypes 5453 P+ (*AvrRph3*), and 200 P- (*AvrRph3*) on seedlings showed that cv. Bowman is susceptible, and BW746 is resistant to *P. hordei* pathotypes 5453 P+ (*AvrRph3*) (Fig. 1*A*) and 200 P- (*AvrRph3*). A single introgressed segment from Estate located on chromosome 7H was detected in BW746 by using genotypic data for 19,593 GBS markers [39]. Fungal infection sites observed microscopically at two days post-inoculation (dpi) in both, cv. Bowman and BW746 were similar in size and morphology (Fig. 1*B*, *SI Appendix*, Fig. SI1*A*). At four dpi, hyphae and haustoria were much more abundant in cv. Bowman than in BW746, whereas symptoms observed macroscopically were similar in both lines (Fig. 1*A* vs 1*B*). At eight dpi, large colonies were formed at many infection sites with urediniospore production initiated in cv. Bowman, whereas infection in BW746 was limited to a few infection sites that developed into small uredinia (Fig. 1*A* vs 1*B*). There was a clear reduction in fungal biomass accumulation in BW746 (Figure 2c). Trypan blue uptake was observed in infected mesophyll cells of BW746 at four dpi showing changes in membrane permeability consistent with cell death associated with the resistance mediated by *Rph3* (*SI Appendix*, Fig. SI1*B*). In contrast, infected mesophyll cells in cv. Bowman showed no detectable change in membrane structure (*SI Appendix*, Fig. SI1*C*). Hypersensitivity in BW746 restricted pathogen development, resulting in chlorotic halos around the infection sites and failure to form large uredinia. F_1 plants of Bowman crossed with BW746 (*Rph3/rph3*) exhibited a slightly higher response than BW746 but were nonetheless much more resistant than Bowman (*SI Appendix*, Fig. SI2), suggesting incomplete dominance in the expression of *Rph3*.

Map-based cloning of *Rph3*. A population of 182 recombinant inbred lines (RILs) from the cross between cv. Scarlett (*Rph3*) and cv. Tallon (*rph3*) was used to investigate the chromosome region encompassing *Rph3* (*SI Appendix*, Table S2). The entire population was genotyped with markers previously reported near the *Rph3* locus in chromosome arm 7HL [40]. Tunable Genotyping-by-Sequencing (tGBS) was used on 42 representative RILs from both resistant and susceptible phenotypic classes (21 lines for each) carrying recombinant chromosomes in the vicinity of the *Rph3* gene, resistant and susceptible bulks each from 10 lines, and the parents identified 24 markers closely linked to the *Rph3* locus and delimited it in a physical window of 4.7 Mb based on the reference cv. Morex genome. Several annotated high-confidence genes evenly distributed within this window were selected to design markers to enrich the genetic map of *Rph3*. After screening 10,411 F_2 individuals from six populations (*SI Appendix*, Table S3, *SI Appendix*, Table S4) with flanking markers MLOC_005 and MLOC_040, 367 recombination events were identified. Phenotyping of the recombinant families delimited the *Rph3* locus to a 0.22-cM interval flanked by markers MLOC_004 and MLOC_023 with 45 recombination events between them (*SI Appendix*, Table S4). Nine additional markers developed in this region (*SI Appendix*, Table S5) based on the reference genome mapped the *Rph3* locus to a 0.02-cM interval between markers MLOC_190 and MLOC_389 with two and three recombinants to the *Rph3* locus, respectively (Fig. 2, *SI Appendix,* Table S6). The three recombinants between MLOC_389 and *Rph3* were confirmed by sequencing (*SI Appendix*, Fig. SI3). The physical

delimitation of the *Rph3* gene was carried out in cv. Barke that has been shown to carry the resistance allele based on the multi-pathotype test in this study (*SI Appendix,* Table S3) and the availability of draft genome sequence [41]. The *Rph3* locus was located in a physical window of 8,519 bp based on the cv. Barke (*Rph3*) genome sequence [41]. This window of 8.5 kb was re-sequenced in all resistant parents from six *Rph3* mapping populations and cv. Barke by the Sanger procedure and demonstrated an identical 8.5 kb sequence without any polymorphisms among all seven resistant lines. There was no annotated gene within the region based on the reference genome annotation for cv. Morex (v2.0 2019) [42] . Manual *de novo* annotation of the 8.5-kb interval of cv. Barke using FGENESH software, identified two open reading frames designated as *ORF1* and *ORF2* (Fig. 2), predicted to encode proteins with 101 and 276 amino acids, respectively.

Forward genetic screen for loss-of-function of *Rph3*-mediated resistance. To determine if *ORF1* and/or *ORF2* were required for the resistance, two ethyl methane sulphonate (EMS) mutagenized populations were produced using two resistant lines, BW746 and cv. Henley (*Rph3*). Six altered phenotype mutant families were identified among 850 M_2 spikes screened with *Rph3*-avirulent pathotype 5453 P- (*SI Appendix*, Table S7). Resequencing of the 8.5-kb *Rph3* region, including *ORF1* and *ORF2* in the six homozygous mutants, revealed four lines with a single nucleotide change in *ORF2*. The two remaining lines without changes within the locus were not allelic with the four known mutants (*SI Appendix*, Table S8). Phenotypic screening of M_3 populations of the four mutants with altered sequences in *ORF2* with an *Rph3* avirulent pathotype confirmed that M198 and M466 were fully susceptible, while M167 and M181 displayed intermediate responses (Fig. 2). Mutant line M198 encoded a truncated protein due to the formation of a new stop codon at position 72, and line M466 had a nucleotide change at the fifth nucleotide in the first intron after the splicing junction. Of the other two mutants, M181 had an L93>F amino acid substitution and M167 had a P126>L substitution. Uredinia formed by the *Rph3*-avirulent pathotype on plants homozygous for each of these latter mutants were significantly larger than those formed on the resistant parents (*SI Appendix*, Fig. SI4). These mutant phenotypes were consistent with changes at the molecular level: alterations in protein structure involving a stop codon (M198) and a predicted splicing variant (M466) resulted in fully susceptible responses. In contrast, the single amino acid substitutions (M167 and M181) resulted in intermediate responses. All these independent point mutations occurred in *ORF2,* and no change was detected in *ORF1* or the intergenic region (8.5 kb physical window) in any of the six altered phenotype mutants. These results demonstrated that *ORF2* is required for *Rph3*-mediated resistance.

Transgenic complementation of *Rph3*. To determine if *ORF2* is sufficient to complement the lack of *Rph3* for resistance to *P. hordei*, we conducted a complementation test using the complete genomic coding sequence of *ORF2* driven by its native promoter. Splice alignment of RNAseq revealed that *ORF2* consisted of an 831 bp coding sequence and 254 bp 5'-, 292 bp 3'- untranslated regions (UTRs). A 7,196-bp DNA fragment containing the entire transcribed region of *ORF2* with the native promoter (3,146 bp upstream region) of the resistant cv. Barke (*SI Appendix*, Fig. SI5) was transformed into the susceptible barley cv. Golden Promise (*rph3*). The T-DNA construct was detected in 16 of 20 primary (T_0) transgenic plants based on PCR results with a selectable marker (*SI Appendix*, Table S9; *SI Appendix*, Fig. SI6). The presence of the transgene in the T_1 generation co-segregated

with a resistant response to the *Rph3*-avirulent pathotype based on a specific marker detecting the *Rph3* resistance allele. The transgenic experiments demonstrated that *ORF2* complemented the lack of *Rph3* in cv. Golden Promise. Taken together, high-resolution and physical delimitation, four independent mutants, and complementation results demonstrated that *ORF2* was *Rph3*.

***Rph3* is induced by *P. hordei* isolates avirulent for *Rph3*.** The *Rph3* transcript was not found in any published barley RNAseq, full-length cDNA, or expressed sequence tag (EST) database. Transcript of *Rph3* was detected in leaves of resistant line BW746 inoculated with *P. hordei* pathotypes avirulent for *Rph3* by RT-qPCR (Fig. 3). In contrast, no transcript was detected in leaves inoculated with either *Rph3*-virulent pathotypes or in mock inoculations (*SI Appendix*, Fig. SI7), which implies *Rph3* is only induced during an incompatible interaction. *Rph3* transcripts were detected in plants of BW746 when challenged with *Rph3*-avirulent pathotypes (200 P- and 5453 P+), but not when inoculated with two diverse *Rph3* virulent pathotypes (5457 P+ and 5656 P+). Transcripts were also not detected in inoculations with the wheat leaf rust pathogen *P. triticina* (pathotypes 26-0 and 104-1,2,3,(6),(7),11,13). These results demonstrate that expression of *Rph3* is induced explicitly by infection with an *Rph3*-avirulent *P. hordei* pathotype (Fig. 3). Moreover, *Rph3* expression was detected only in infected tissue, indicating that a signal could not be transmitted to non-infected parts of the same plant (*SI Appendix*, Fig. SI8). Expression was not detected for any *Rph3* homolog in the susceptible haplotype (cv. Morex) during infection regardless of the rust pathogen used (*SI Appendix*, Fig. SI9). Similarly, transcripts of the putative *ORF1* were not detected in any treatments. Taken together, these experiments showed that *Rph3* is expressed explicitly in barley genotypes carrying the *Rph3* resistance allele, only when challenged with an *Rph3*-avirulent *P. hordei* pathotype and that upregulation of the gene occurs exclusively in infected tissue.

Bioinformatic and phylogenetic analysis of the *Rph3* gene family. BLAST searches of RPH3 amino acid sequences against the National Center for Biotechnology Information revealed no matches to the Conserved Domain Database (CDD v3.18 - 55570 PSSMs) using the default expected (E)-value. This suggests that this protein is highly divergent among different plant species, lineage-specific, or not annotated due to a lack of molecular evidence such as RNAseq. RPH3 secondary structure predictions from three independent programs (TMHMM, TMPRED, and Protter) suggested an insoluble protein comprising 5 to 7 transmembrane helices (*SI Appendix*, Fig. SI10), indicating that RPH3 is likely an integral membrane protein.

A BLASTX search against the non-redundant database using the cDNA of *Rph3* as a query returned seven hits with different levels of identity. The 9-cis-epoxycarotenoid dioxygenase (HORVU_NCED) protein from barley shares 46% identity with RPH3. Two sequences with similarity to RPH3 were retrieved from *Aegilops tauschii,* consisting of LOC109787323 and LOC109787282, and one from *Brachypodium distachyon,* Bradi1g31183.3. No ortholog was identified in *Brachypodium stacei*, suggesting that this gene family experiences gene loss in independent lineages. BLASTN against the reference genome of various crop species revealed homologs of *Rph3* in each of the three genomes A, B, and D of bread wheat (*Triticum aestivum*), and one homolog in oat (*Avena sativa*). BLASTN against the barley Morex v2.0 reference genome [42] found seven similar sequences, all located within 98.8 kb flanked by markers MLOC_190 and MLOC_389 in chromosome arm 7HL. These seven similar

sequences indicate four putative homologous genes of *Rph3,* namely *HORVU_ORF5*, *HORVU_ORF10*, *HORVU_ORF11*, and *HORVU_ORF12*. Sequence similarities are described in *SI Appendix*, Fig. SI11 figure legend.

The phylogenetic relationship between the RPH3 protein and the four cereal homologs suggests that the RPH3 protein evolved the ability to confer resistance against *P. hordei* within barley after the divergence of wheat and barley (*SI Appendix*, Fig. SI11*A*). However, putative orthologues could be involved in disease resistance in the related species. Analysis of motif composition of RPH3 and its homologs/paralogs using the Surveyed conserved motif ALignment diagram and the Associating Dendrogram (SALAD) showed eight conserved motifs (*SI Appendix*, Fig. SI11*A*), and seven transmembrane helices overlapped all of these motifs except for motifs 5 and 8. Among all, motifs 1-3 were present in almost all related proteins, of which motif 1 has two N-myristoylation sites, one phosphorylation site of protein kinase C, and two phosphorylation sites of casein kinase II (*SI Appendix*, Fig. SI11*B*). Although considerably larger than RPH3 (276 aa), the wheat homolog TraesCS7D_RPH3_LIKE (401 aa) located on chromosome 7D shares all motifs with RPH3 and in the same order, suggesting they are orthologs.

Grass species diverged from a common ancestor about 60 million years ago [43] and have considerable variation in chromosome number, genome size, and sequence. However, most of the genes present in grass species are conserved, and the gene order among them is mainly collinear [44,45]. The long arm of barley chromosome 7H that harbours *Rph3* is syntenic with the long arm of chromosome 7 in the wheat A, B, and D genomes [46]. We showed that micro-synteny is well conserved in the vicinity of *Rph3* between barley and wheat genomes (*SI Appendix,* Fig. SI12). Orthologs of the *Rph3* gene were found in the wheat A, B, and D genomes within the expected locus, of which the copy from the D genome has motifs in identical order to RPH3 and the two proteins share 88% similarity at the amino acid level (*SI Appendix*, Fig. SI11A). Four loci conferring resistance to wheat leaf rust on one or other long arm of wheat chromosome 7 have been designated, namely *Lr14a-b* (7BL), *Lr19* (7DL), *Lr20* (7AL), and *Lr68* (7BL) [47-50]. Among these loci, *Lr68* confers adult stage resistance while the other three loci confer all-stage resistance. None of these genes is located in a region homologous to the *Rph3* gene (*SI Appendix*, Fig. SI12). This suggests that either *Rph3* gained a role in immunity post divergence, or alternatively, insufficient sampling has been performed in Triticeae species to identify functional orthologs.

Rph3 **induces cell death in** ***N. benthamiana.*** The expression of *Rph3* in the presence of the corresponding avirulence gene but apparent lack of expression when avirulence is lacking is reminiscent of executor gene resistance to *Xanthomonas* spp. conferred by genes such as *Bs3* [51], *Xa10* [52], *Xa23* [53], *Xa27* [54], and *Bs4C* [55]. We performed heterologous expression of *Rph3* in *N. benthamiana* to assess whether RPH3 acts as an executor protein and found that it caused cell death when transiently expressed under the *MasΩ* promoter (Fig. 4). This cell death phenotype was comparable to that induced by overexpression of *Xa10* [52], *Xa23* [53], and *Bs4C* [55] and known to cause cell death in *N. benthamiana.* Previously, heterologous expression of *Xa27* was not shown to cause cell death in *N. benthamiana* [54]. We found that this absence of cell death is likely dependent on expression level, as the *MasΩ* promoter was sufficient for *Xa27*-mediated cell death in *N. benthamiana* (Fig. 4*A*). Expression of *rph3* alleles identified from the loss-of-function mutagenesis screen indicated that early truncation mutant

M198 (E72*) did not cause cell death, whereas the non-synonymous mutants M167 (L93F) and M181 (P126L) caused cell death in *N. benthamiana* (Fig. 4*B*). This result matched quantitative phenotyping results of the mutants, where mutant M198 (E72*) has the most significant effect on resistance showing complete susceptibility, whereas mutants L93F and P126L are partial loss-of-function with reduced level of resistance.

Transcription dynamics of *Rph3*-mediated resistance at two days post-inoculation. We performed RNAseq analysis of cv. Bowman and BW746 to measure the response of barley to *P. hordei* in the presence and absence of *Rph3* two days after inoculation with *P. hordei* or the application of oil (mock). Differentially expressed genes were identified for every pairwise comparison of genotype and treatment using a false discovery rate of 5%. In mock-inoculated conditions, 5,465 differentially expressed genes (DEG) were identified between cv. Bowman and BW746, indicating that a considerable number of genes are differentially expressed between these barley accessions at steady-state levels. Volcano plots showed that most expression differences were minor and likely associated with genetic differences between cv. Bowman and BW746 and their interaction with the oil medium used for mock inoculation. In *P. hordei* inoculated leaves, there were 4,841 DEG for cv. Bowman versus BW746, and for mock-inoculated versus *P. hordei*-inoculated cv. Bowman, there were 4,873 DEG. The number of DEG between mock and *P. hordei*-inoculated in BW746 was 8,762 (*SI Appendix*, Fig. SI13). RNAseq reads for *Rph3* were detected in two of three replicates of BW746 inoculated with *P. hordei* and not seen in any other treatment. More genes were differentially expressed in the incompatible interaction among treatments than in the compatible interaction at two days post-inoculation. This comparison also produced the most significant number of unique differentially expressed genes among treatment comparisons (3,004 DEG). Gene ontology enrichment analysis found that up-regulated genes are associated with several biological processes related to transport, such as vesicle-mediated (p_{adj}=8.4e-25) and protein transport (p_{adj}=5.2e-15). In contrast, enrichment in down-regulated genes was localized to the plastid (p_{adj}=7.5e-36) and associated with photosynthesis (p_{adj}=2.1e-4) (*SI Appendix,* Table S10). This indicates that *Rph3*-mediated resistance is correlated with up-regulation of endomembrane trafficking components, which might contribute to the immune response.

Allelic variation in *Rph3*. The *Rph3* region located between MLOC_190 and MLOC_389 in the susceptible barley cv. Morex encompasses a physical interval of 98,478 bp compared to 8,519 bp in the resistant cv. Barke (*SI Appendix,* Fig. SI14*A*, *B*). Four homologous sequences of the *Rph3* gene were found in cv. Morex (*SI Appendix,* Fig. SI14*C*). All four *Rph3* homologs encode proteins of unknown function. The BLASTN of the *Rph3* gene against the whole genome of cv. Barke revealed only one hit in the barke_contig_512435, the *Rph3* gene. A primer pair based on the draft reference genome sequence of cv. Barke [56] was designed to amplify the complete coding and intron sequences of *Rph3* (*SI Appendix,* Table S11). These primers were applied to a collection of 78 barley accessions comprising 41 lines with and 37 without *Rph3* and representing all known *Rph3* alleles, including *Rph3.c*, *Rph3.aa*, and *Rph3.w* [57]. A perfect correlation between these PCR primers and *Rph3* gene postulation was found. All 41 lines postulated to carry *Rph3* genes were PCR positive, and all 37 lines postulated without *Rph3* were PCR negative for the designed primers (*SI Appendix*, Table S12). The alignment showed that the entire

DNA sequence was identical among all resistant accessions. This finding suggests a monophyletic origin of *Rph3* within cultivated barley. The responses of three Bowman NILs carrying three different postulated alleles of *Rph3* to pathotype 5453 P+ (avirulent for *Rph3*) of *P. hordei* were the same (*SI Appendix,* Fig. SI15). Therefore, we conclude that all of these stocks originated from the same ancestor and transcribed one unique isoform of *Rph3*.

Analysis of GBS markers using a worldwide barley collection of 20,607 accessions identified a single paired GBS marker landing on the *Rph3* gene. This paired GBS marker (gRph3_I1E2 and gRph3_E2I2; *SI Appendix*, Table S13) was detected in 134 accessions comprising 32 landraces, 70 cultivars, 14 breeding lines, 15 wild accessions, one semi-wild accession, and two other genotypes (*SI Appendix*, Table S14). The landraces and breeding lines with *Rph3* were from many parts of the world, but the cultivars were mostly from Europe (especially Germany with 27 accessions). The wild accessions were collected in Israel (9 accessions), Syria (8 accessions), Jordan (2 accessions), Greece (2 accessions), or had unknown origins (4 accessions) [58]. Haplotypes identified with this approach had an identical sequence for the GBS markers. This GBS marker was applied to the 314 Wild Barley Diversity Collection (WBDC) population and identified ten accessions carrying *Rph3* (*SI Appendix,* Table S15) [59]. Simultaneously, a dominant marker (MLOC_400, *SI Appendix,* Table S5) based on the *Rph3* gene sequence confirmed the presence of dominant *Rph3* allele in all ten accessions carrying the GBS marker and identified five additional accessions (WBDC044, WBDC094, WBDC238, WBDC254, and WBDC260) (*SI Appendix*, Table S15). Sequence alignment of GBS markers for the five WBDC accessions not previously identified in the k-mer analysis found 8 to 9 SNPs relative to *Rph3*. Three additional haplotypes were identified as Hap2: WBDC094 and WBDC254; Hap3: WBDC238 and WBDC260; and Hap4: WBDC044. The identification of multiple sequence variations within wild barley suggests that additional allelic variants of *Rph3* may exist. These findings also indicated that the *Rph3* gene likely originated from wild barley in Israel, Syria, Jordan, or Greece, from which it was introgressed into cultivated barley germplasm.

Discussion

Here, we have identified the gene underlying *Rph3*-mediated resistance to *P. hordei* using map-based cloning, mutagenesis, and transgenic complementation. This gene is exclusively expressed when the plant is attacked by avirulent pathotypes and expression of *Rph3* triggers cell death in barley and *N. benthamiana*. The *Rph3* gene encodes a small protein of 276 amino acids with multiple predicted transmembrane helices and contains no conserved domains of any resistance protein families known to date. The expression profile and structural characteristics of the encoded protein suggest that *Rph3* acts as an executor gene. The executor genes that have been reported to date are involved in resistance to bacterial diseases in rice and pepper, and here we report *Rph3* as a potential executor gene against a fungal disease in cereals.

The inducible expression of *Rph3*. Most cloned disease resistance genes are expressed constitutively [60,61]. Constitutive expression was observed in genes conferring resistance to various pathogens, including bacteria [62-64] and fungi [65-68]. However, expression of some resistance genes is induced by an external factor, and this group can be divided into two subgroups. The first subgroup consists of genes whose expression is induced by an avirulent pathotype, a virulent pathotype, or physical damage. Two examples of this are *Xa1*, which confers resistance to *Xanthomonas oryzae* in rice and *Ve1*, which confers resistance to *Verticillium dahlia* strain Vd1 in tomato. These two genes are induced upon pathogen infection irrespective of pathogenicity, as well as by physical damage [65,69]. The second subgroup consists of genes whose expression is induced exclusively in the presence of avirulent strains or pathotypes. This phenomenon has been reported for genes conferring resistance to plant viruses, bacteria, and fungi, and the barley gene *Rph3* belongs in this sub-group.

A particular induction of a resistance gene to an avirulent pathogen in the last sub-group has been observed in only a few systems [53,70]. Expression of the *N* resistance gene in tobacco was induced by TMV infection but not by Potato Virus Y [71]. Induction by an avirulent pathotype only has been documented for genes conferring resistance to fungal pathogens, including the barley mildew pathogen *Blumeria graminis* f. sp. *hordei* [72], the sunflower downy mildew pathogen *Plasmopara halstedii* [73], and the rice blast pathogen *Magnaporthe oryzae* [74]. The most well characterized class of resistance genes in this group are the rice genes *Xa7, Xa10*, *Xa23*, and *Xa27,* conferring resistance to the bacterial pathogen *X. oryzae* pv. *oryzae*, and the pepper genes *Bs3* and *Bs4C* conferring resistance to *X. campestris* pv. *vesicatoria*. These *Xanthomonas* resistance genes are activated by corresponding transcriptional activator-like effectors (TALE) secreted by avirulent strains [51,53,54,75]. TALE-activated resistance genes were designated "executor" genes as they are solely involved in triggering a plant immune response [76]. In this study, the *Rph3* gene is expressed only upon infection with an avirulent genotype of *P. hordei*. Like *Rph3*, all currently cloned executor genes encode transmembrane proteins. The similarity in both expression profile and transmembrane domains suggests a similar resistance mechanism. We hypothesize that *Rph3*-avirulent *P. hordei* pathotypes produce an effector, *AvrRph3*, that directly or indirectly triggers expression of the *Rph3* gene. Further work is required to demonstrate this, in particular, the isolation of *AvrRph3*. It will be critical to determine whether AvrRph3 has the capacity to bind DNA and specifically interact with the promoter of *Rph3* or alternatively, if AvrRph3 induces *Rph3* expression

through earlier transcriptional components such as transcription factors, the Mediator complex, or RNA polymerase II.

Effectors secreted by pathogens target host proteins to enhance infection. On the other hand, plants evolved resistance genes with promoter sequences that target effector proteins to initiate defence response, including cell death. This co-evolutionary process has led to host decoy genes, the proteins of which mimic an operative effector target to intercept the pathogen effector [77]. In plant-*Xanthomonas* spp. interactions, genes encoding executor proteins that facilitate an immune response that routinely includes cell death gained promoter sequences similar to host virulence targets. In this context, the promoter of the executor acts as a decoy to the original host target [77]. This model suggests that executors only function when pathogen effectors are present, do not contribute to pathogen fitness in the absence of the cognate R protein, and potentially have an exclusive role in plant immunity [77]. Among the executor genes mentioned above, the *Bs3* gene was suggested to function as a decoy. To date, no other function has been associated with the pepper *Bs3* gene rather than resistance to *Xanthomonas*. Inactivity of the *Bs3* gene in the absence of the *AvrBs3* effector supports its exclusive biological function [51]. AvrBs3 targets several promoters, including the promoter of gene *Upa20* [78]. AvrBs3-mediated expression of *Upa20* leads to misregulation of cell size in pepper (hypertrophy) [78]. Notably, both *Bs3* and *Upa20* have the same promoter element, an *upa*-box (TATATAAACCN$_{2\text{-}3}$CC), which is targeted by the AvrBs3 effector [51]. In this case, the promoter of the *Bs3* gene acts as a decoy that mimics the target of *AvrBs3* (promoter of *Upa20*), and based on that, traps this effector and activates transcription to trigger the defence response. The *Rph3* gene may not have any function in the absence of an *AvrRph3* effector as we could not detect its expression among publicly available barley RNAseq databases. Although neither the AvrRPH3 protein nor the operative target of this protein was identified, the similar expression pattern between *Rph3* and *Bs3* indicates that they may work similarly. Further work is required to determine if *Rph3* is expressed in a unique developmental context or whether it has an exclusive role in plant immunity.

Molecular function of the RPH3 protein. Plants have evolved proteins that recognize pathogen attacks and trigger immune response pathways to defend against invaders upon pathogen detection [79]. Of the 19 resistance genes isolated from wheat and barley that confer race-specific rust resistance, 17 encode NLR proteins [5,80,81], one of the largest and most diversified plant disease resistance gene families [82,83]. The exceptions are stem rust resistance genes *Rpg1* from barley [84] and *Sr60* from diploid wheat, both of which encode proteins with two kinase domains in tandem [80]. The *Rph3* gene is a new class of resistance genes that shows no similarity to any of these genes. The RPH3 protein is predicted to contain five to seven transmembrane helices depending on the prediction tools. The genes *Lr34* and *Lr67* conferring leaf rust resistance in wheat [16,17], and *Xa7*, *Xa10*, *Xa23*, *Xa27,* and *Bs4* (executor genes) conferring resistance to *Xanthomonas* sp. in rice and pepper [70,85], also encode proteins with multiple transmembrane helices. While *Lr34* and *Lr67* are race-non-specific, executor genes are race-specific. Cloned executor genes encode small proteins (113 – 342 aa) that are predicted to contain transmembrane helices [52-54,75,85]. The Bs3 protein shows a high level of similarity to flavin monooxygenases [76], whereas the other executor proteins and RPH3 showed no significant sequence homology to any known

resistance protein [53,85]. Our study demonstrated that the RPH3 protein appears to cause cell death in barley and in the heterologous system *N. benthamiana*. The cell death can be directly prompted by Rph3 protein or indirectly via triggering a defence pathway. Previous work has shown that the executor genes (*Xa7*, *Xa10*, *Xa23*, *Bs3*, and *Bs4C*) trigger cell death in both their host (rice or pepper) and *N. benthamiana* [51-53,75,85]. Although *Xa27* was reported to triggers cell death only in rice [54], we found that it does trigger cell death in *N. benthamiana* when driven by the *MasΩ* promoter, suggesting that expression level is essential for function. XA27 was found in the apoplast, whereas other executor proteins were localized in the endoplasmic reticulum [52,53,75,76,86]. Furthermore, executor genes trigger programmed cell death in different ways; for example, Bs3 causes cell death via the accumulation of salicylic acid and pipecolic acid [76], whereas cell death attributed to XA10 and XA23 is related to cellular Ca^{2+} homeostasis. The mechanisms underlying cell death mediated by BS4C, XA27 and RPH3 remain unknown. The typical features of RPH3 and known executors, including similar expression patterns, small proteins with predicted transmembrane helices, and cell death induction, suggesting that the RPH3 protein is an executor. To date, executor genes conferring resistance to a fungal pathogen have not been reported before.

The RPH3 protein showed 46% amino acid similarity to 9-cis-epoxycarotenoid dioxygenase (NCED), an enzyme with catalytic activities reportedly involved in response to abiotic stresses such as drought [87], salt and water-logging [88], or multi-abiotic stresses [89], via biosynthesis of abscisic acid (ABA). ABA plays a vital role in controlling stomata closure in angiosperm species in response to high vapour pressure [90], and its biosynthesis is regulated by the *NCED* gene [91,92]. ABA is also known to prevent bacterial invasion by regulating stomatal closure [93]. It was found to be involved in resistance to *Rhizoctonia solani* by impairing host cellulose synthesis [94,95] and in resistance to wheat rust pathogens mediated by resistance gene *Lr34* [96]. Based on the protein similarity of RPH3 and NCED, the involvement in ABA biosynthesis in *Rph3*-induced resistance to *P. hordei* can be hypothesized. Functional studies are required to test this hypothesis and to decipher the molecular role of the unknown RPH3 protein.

Origin of *Rph3*. Wheat and barley originated in the Fertile Crescent [97,98]. It is well demonstrated that cultivated barley (*Hordeum vulgare* ssp. *vulgare*) derived from its immediate wild progenitor (*H. vulgare* ssp. *spontaneum*) several times in the region spanning modern-day South-east Turkey, Syria, Jordan, and Israel [99]. As farming expanded, these derivatives spread throughout Europe, Asia, and Africa [99].

Major bottlenecks in genetic variation in many crops were caused by domestication and many variations remained in the wild gene pool [100,101]. Wild barley that freely crosses with cultivated barley is a well-known source of allelic variation [102,103]. The *Rph3* gene is a functional allele that confers resistance, and its semi-dominant behaviour can be accounted for as a gene dosage effect. Resistant and susceptible alleles could result from a point mutation (loss of function or gain of function), gene duplication followed by neofunctionalization (gain of function), or be of independent origin (unequal recombination, insertion, deletion, or inversion). The significant differences in the structure between the resistant (*Rph3*) and susceptible (*rph3*) alleles at the DNA level (8.5-kb vs 98.5-kb) plus many nucleotide substitutions within the causal gene (37 SNPs between the coding

sequence of *Rph3* and its most similar gene *ORF10*) imply ancient, independent origins. The *Rph3* resistance allele was detected based on sequence analysis in wild barley accessions collected from the Eastern Mediterranean and Greece. The gene in modern cultivars originated from two donors, cv. Aim and landrace Estate, both of which are spring type, six-rowed, and came from Egypt [22,104]. The two lines are accessioned as HOR 2470 and HOR 2476 in the barley collection at IPK, and their pedigrees are unknown. The best explanation would be that the gene was introgressed into cultivated barley from wild barley in or around Egypt via hybridization. This hybridization could have been a result of deliberate crossing by a farmer/breeder to introduce a new beneficial allele or random outcrossing between a cultivar and wild relatives growing as a weed in the vicinity followed by deliberate selection by a farmer. It is impossible to separate these hypotheses due to the lack of information about the origin of both accessions. The sequence identity of *Rph3* among all 41 resistant lines of cultivated barleys from diverse sources indicates a single introgression event. Of interest, the alleles *Rph3.c*, *Rph3.aa*, and *Rph3.w* were designated based on differing origins [57] all show identical specificity with Australian isolates of *P. hordei* and all were found to share 100% sequence identity.

Analysis of variation in the *Rph3* allele in wild barleys collected from different geographical areas may allow discovering other functional alleles of *Rph3*, allowing direct mining of genetic diversity to discover new resistance alleles to protect barley from *P. hordei*. Identifying five wild barley accessions carrying polymorphisms in a GBS marker tightly linked to *Rph3* suggests that additional alleles of *Rph3* may exist in (wild) barley. Further genotypic and phenotypic characterization of genetic diversity is required to determine if these represent novel functional alleles with different specificities or are equivalent to *Rph3*. The evolution of the *Rph3* gene can be further investigated by examining its conservation across species within the Triticeae, and if possible, other Poaceae species to identify the origin of this protein family.

Cloning studies have shown that non-durable resistance genes tend to be NLRs. The current study demonstrates that other types of resistance genes are also vulnerable to evolving pathogens and that much remains to be learnt about the durability of resistance genes. This study showed that *Rph3* transcription is induced only by avirulent *P. hordei* pathotypes. *Rph3* encodes a transmembrane executor that induces host cell death in similar manner to rice *Xa7, Xa10, Xa23, Xa27* and *Bs3* and *Bs4c* in pepper. The existence of an executor gene in cereals conferring resistance to *P. hordei* raises the possibility that the fungus encodes an effector that has similar activity as TAL effector-like proteins, or alternatively, targets other components of the plant transcriptional machinery that precisely activates *Rph3* expression. With breakthroughs in gene engineering, the isolation of *Rph3* provides an additional resistance gene to include in transgenic cassettes for gene pyramiding. This study suggested that the *Rph3* gene has a single origin in the cultivated gene pool and was introgressed from a wild barley probably collected from Israel, Syria, Jordan, or Greece into the cultivated gene pool relatively recently. Furthermore, engineered executor genes in rice and pepper that contained additional TAL- effector binding sites showed increased resistance specificity. If *Rph3* gene induction is also due to the binding of TAL-effector like proteins to the promoter a similar strategy could be used to increase the resistance specificity of this protein to other *P. hordei* strains or other plant diseases.

Materials and Methods:

Materials. We phenotyped and genotyped RILs, F_2, mutant, and transgenic populations segregating for *Rph3* using various *P. hordei* pathotypes with different pathogenicities as described in SI Appendix, SI Materials, and Methods.

Methods. Experimental procedures of histology, DNA isolation, gene mapping, mutant screening, allelism test, gene transformation, transient assay, gene evolution analysis, genetic diversity analysis, phylogenetic analysis, expression analysis using RT-qPCR, and RNAseq analysis were conducted as described in SI Appendix, SI Materials and Methods.

Data availability. RNAseq data have been deposited in Sequence Read Archives at National Center for Biotechnology Information (NCBI) under BioProject accession number PRJNA731362. The full-length cDNA and genomic sequence of the *Rph3* gene have been deposited in NCBI with the accession number MZ561688 and MZ561689.

ACKNOWLEDGMENTS. We thank Prof. R. A. McIntosh for suggesting the experiment that assessed the tissue specificity of *Rph3* expression; Dr. P. Zhang for help in seed mutation; Dr. C. Dong and Ms. M. Demers for assistance with RNA extraction; Dr. E. Wang for help with RT-qPCR; Dr. P. Dracatos for discussion related to mutant analysis; Dr. E. Lagudah for discussion on protein function; Prof. S. Ho for suggestions related to phylogenetic analysis; Mr. M. Williams for technical support with plant growth facilities; Mrs. S. Sommerfeld for assistance in generating transgenic barley plants; Mrs. K. Niedung for technical support with artificial inoculation, DNA extraction and PCR on transgenic materials; Dr. I Hernández-Pinzón for technical support with PCR on wild barley germplasm; GRDC, Gatsby Foundation, and UKRI-BBSRC (BBS/E/J/000PR9795) for financial support; and the Australian Awards Scholarship for providing financial support to HD.

SI Materials and methods

Histology and fungal biomass

Histology. The procedure followed Ayliffe et al. 2011 [105] with slight modifications. Segments of 3-4 cm of first leaves from cv. Bowman and BW746 inoculated with the *P. hordei* pathotype 5453 P+ were harvested at 2 dpi, 4 dpi, and 8 dpi. The collected leaf samples were autoclaved in 50-ml screw-cap tubes containing 25 ml of 1 M potassium hydroxide (KOH) at 121°C for one hour to remove chlorophyll. After autoclaving, the KOH solution was gently removed, and the leaf samples were twice gently washed with Tris-HCl (50 mM, pH 7.0) before adding 10 ml of the same Tris buffer to neutralize the samples. Before staining, most of the Tris buffer was removed to leave the tissue in minimum volume. A 1-mg/ml solution of WGA-FITC was added to the tissue to produce a final stain concentration of 20 µg/ml. The samples were stained for one hour before microscopy using a Zeiss Axio Imager confocal microscope (Zeiss, Germany) with 488-nm excitation and 510-nm emission wavelength.

Quantification of fungal biomass in infected tissues. Quantification of fungal biomass was performed by chitin measurement as described by Ayliffe et al. [106]. Infected leaf tissues from four biological replicates of cv. Bowman and BW746 were harvested at 2, 4, and 8 dpi, weighed and placed in 15-ml Falcon tubes. One M KOH containing 0.1% Silwet L-77 (Lehle Seeds, U.S.A.) was added to cover the tissue entirely. After autoclaving, the tissues were washed and neutralized as described in the "histological analysis" section. Subsequently, the liquid was poured off and replaced by 1 ml of Tris (pH 7.0) for each 200 mg of plant tissue. The plant tissue was macerated by sonication for 1 minute to produce a fine, uniform tissue suspension. Each sample was stained with WGA-FITC (Sigma Aldrich) dissolved in water by repetitive pipetting before being left to stand for 10 minutes at room temperature. Samples were then centrifuged at 600 × *g* for 3 minutes. The supernatant containing unbound stain was removed by pipetting, and the pellet was resuspended in 200 µl of 50 mM Tris (pH 7.0). Samples were washed three times in 200 µl of 50 mM Tris (pH 7.0) before resuspension in 100 µl of 50 mM Tris (pH 7.0) and transferred to black, 96-well microtiter trays for fluorometry. Fluorometric measurements were made with a Wallac Victor 1420 multilabel counter (Perkin-Elmer Life Science, U.S.A.) fluorometer with 485-nm adsorption, 535-nm emission wavelength and 1.0-sec measurement time.

Cloning of the *Rph3* gene

Pathogen materials. Four *P. hordei* pathotypes designated according to the octal notation proposed by Gilmour (1973) [107] (*viz.* 200 P- [Plant Breeding Institute culture number 518], 5453 P+ [584], 5457 P+ [612], and 5656 P+ [623]) and two *P. triticina* pathotypes (26-0 [111] and 104-1,2,3,(6),(7),11,13 [547]) were used in this study. Pathotype 5453 P+ was used for phenotyping recombinants and screening mutants, all six pathotypes were used for gene expression, and the first three *P. hordei* pathotypes were used for multi-pathotype analysis. The suffix P+/P- added to each octal designation indicated avirulence/virulence for resistance gene *Rph19* [108]. These pathotypes were originally raised from single uredinia on the leaf rust susceptible genotype cv. Gus in the greenhouse and the urediniospores were dried above silica gel for 5-7 days at 12 °C before being stored in liquid nitrogen at the Plant Breeding Institute, the University of Sydney, Australia. Details for each pathotype, including pathogenicity on different resistance genes, are listed in the *SI Appendix,* Table S16.

Phenotypic analysis. At around eight days after sowing and just prior to second leaf emergence, the seedlings were inoculated with urediniospores suspended in light mineral oil (IsoparL®, Univar, NSW, Australia), at a rate of approximately 10 mg of spores per 10 ml oil per 200 pots. The suspension was atomized over seedlings in an enclosed chamber using a hydrocarbon propellant at ambient temperatures. The inoculated plants were incubated in a misted dark room (20 – 22 °C), with mist generated by an ultrasonic humidifier for 18 hours and moved to a temperature-controlled microclimate room maintained at 23 °C under natural light. The rust responses of at least ten independent seedlings for each line were recorded at 8 - 10 days post-inoculation using the "0"– "4" infection type (IT) scale [109] with cv. Gus as the susceptible control. IT scores vary from complete immunity "0" without any visible symptoms to full susceptibility "4" with large uredinia without

chlorosis. The letters "c", "n" indicated chlorosis or necrosis. The symbols "-" or "+" indicated lower or higher infection types than usual. An IT of 3 or higher was interpreted as susceptible; further details are provided by Park and Karakousis [110].

Plant materials and growth conditions. The basic map of the *Rph3* locus was generated using 182 recombinant inbred lines (RILs) derived from the cross cvs. Scarlett (*Rph3*) x Tallon (*rph3*). Based on the genotypic and phenotypic data (*SI Appendix*, Table S2), a subset of 42 lines, one resistant and one susceptible bulk of 10 samples each carrying recombination events adjacent to *Rph3*, and the two parents were chosen for genotyping using selected tGBS markers. A high-resolution genetic map of the *Rph3* locus was constructed based on pooled data for 10,411 F_2 plants derived from six segregating populations (*SI Appendix,* Table S4). The segregants were genotyped using DNA markers flanking the *Rph3* locus (MLOC_005 and MLOC_040). Progeny in which a recombination event had occurred between these markers were further genotyped using internal DNA markers to define the recombination site. All recombinants were self-pollinated to select homozygous recombinants using appropriate DNA markers, and the homozygotes were challenged with *Rph3*-avirulent *P. hordei* pathotype 5453 P+ and were scored for rust response based on our phenotyping platform to have unequivocal phenotypic data. Additionally, homozygous recombinants scored for all internal DNA markers.

An international barley collection of 78 accessions representing different sources and alleles of *Rph3* based on previous research was subjected to multi-pathotype tests to study the allelic variation (*SI Appendix*, Table S12). Each accession was initially been multiplied from a single seed to ensure genetic purity. Genotypic and phenotypic data were collected from each pure line.

DNA isolation and marker analysis. F_2 seeds were sown in 96-punnet (12 x 8) trays filled with potting mix. At the 8-day-old stage after the emergence of the second leaf, about 30 mg of the first leaf of each seedling was sampled into a 96-well collection tube (12 x 8 wells) containing two ball bearings and subjected to DNA extraction using an SDS method. To stabilise the DNA, 450 µl of extraction buffer including 0.1 M of Tris-HCl buffer (pH 8.0), 0.005M EDTA buffer (pH 8.0), 0.5M NaCl, 2-Mercaptoethanol (70 µl/100 ml buffer), and RNAse (100 µg/ml) were added to each sample before crushing. A TissueLyzer II (Qiagen, Germany) at 25 Hz for 2 minutes was used for crushing the leaf material in the extraction buffer. The final mixture was then added with SDS solution (1.2% final concentration) to solubilize the proteins and lipids at 65°C for 60 minutes. The remaining proteins were precipitated by adding ammonium acetate 7.5 M to reach a final concentration of 2 M. The mixture was incubated at 4°C for 60 minutes, followed by centrifuging at 4,800 rpm (4,327 ×g) for 10 minutes to separate debris and the aqueous phase. The upper phase containing genomic DNA was transferred to a new 96 well format plate and pelleted out by adding 100 µl of chilled isopropanol to 100 µl of supernatant. The pellet was twice washed using 100 µl of 70% ethanol before being slowly dissolved in 200 µl TE 0.1x buffer for six hours for downstream applications.

Primer3Plus software (http://www.bioinformatics.nl/cgi-bin/primer3plus/primer3plus.cgi) was used to design PCR primers that were subsequently synthesized commercially (Sigma Aldrich, Australia). Each 10 µl PCR contained 0.2 units of high-fidelity DNA polymerase (MyFi™, Bioline, Australia), 0.3 µM of each primer, 1x MyFi reaction buffer (Bioline, Australia), and 20 ng of genomic DNA. Thermocycling conditions consisted of an initial denaturation of 95°C for 10 minutes followed by 30 cycles of 94°C for 30 seconds, 55-60°C for 30 seconds, 72°C for 30 seconds, followed by a final extension at 72°C for 10 minutes. PCR products were digested (using a suitable endonuclease when required (*SI Appendix*, Table S5)) for three hours under the recommended temperature. The digested products were monitored by electrophoresis on an agarose gel and visualized by staining with 6x GelRed® (Biotium, USA) (1.5 µl/100 ml agarose gel).

Physical mapping. The sequences of high-confidence genes and non-repetitive sequences on Chr. 7HL extracted from the IPK Barley server (https://webblast.ipk-gatersleben.de/barley_ibsc/viroblast.php) were selected to develop markers to construct a high-resolution map of the *Rph3* locus. The sequence of each marker generated for parental lines by Sanger sequencing was used to do homology searches against the Barley Pseudomolecules Masked Apr2016 library to determine its physical position. Parental sequences were aligned with ClustalW within the MEGA-X software [111]. Polymorphic restriction endonuclease sites were identified by the dCAPS tool at http://helix.wustl.edu/dcaps/dcaps.html. The sequences of the closest flanking markers MLOC_190 and MLOC_389 were used to determine the physical window of the *Rph3* locus in the genome database of barley cvs. Morex and Barke [41].

Candidate gene validation by EMS-induced mutants

Generation of mutant populations. Seed of cv. Henley (*Rph3*) and BW746 (*Rph3*) were treated with ethyl methane sulphonate (EMS) according to Caldwell et al. (2004) [112] with some modifications. Nine batches of barley seeds comprising 1,200 and 1,500 seeds of cv. Henley and BW746 were imbibed in a 2,000-ml glass flask filled with one liter of deionized water for four hours at ambient temperature. The water was then replaced by 500 ml of 16 mM EMS (0.2%) solution, and the flask was gently shaken for 20 hours at ambient temperatures. After treatment, the seeds were extensively washed under running water for two hours. Subsequently, the seeds were transferred to trays covered with Whatman paper and placed in a fume hood for slow drying (about 16 hours) before sowing. The treated seeds were sown directly in the field. After four weeks, the seedlings were thinned randomly to about ten plants/meter. Approximately 400 spikes of cv. Henley and 600 spikes of BW746 were harvested from 300 M_1 plants of each.

Mutant screening. In total, 350 and 500 M_2 single heads from cv. Henley and BW746, respectively, were used for gene validation. The M_2 spikes and selected M_3 families were screened for knockout mutants using the *Rph3*-avirulent pathotype 5453 P+. Each M_3 line was sown in an independent pot and tested for rust response. All the

susceptible and three resistant plants were transplanted for each family showing a segregating reaction. The *Rph3* locus (8,519 bp in length) in M_3 susceptible plants was resequenced using the Sanger method. The M_3-derived M_4 families were progeny-tested to confirm the phenotype of M_3 plants.

Allelism test. The EMS-induced mutants were divided into two groups. Group I included mutants with nucleotide changes within the *Rph3* locus, and Group II consisted of mutants with no nucleotide change within the locus (8.5 kb). Three types of crosses were made to test the allelism of the EMS-induced mutations: Group I x Group I; Group I x Group II; Group II x Group II. The F_1 seeds and their parents were inoculated with *P. hordei* pathotype 5453 P+ to test the allelic status of these mutants (*SI Appendix,* Table S8).

Validation of the candidate gene by complementation test

***Rph3* construct.** A genomic DNA segment of 7,096 bp sequence including 2,196 bp sequence of the gene *Rph3*, 3,400 bp of upstream sequence including the 5'-UTR region, and 1,500 bp downstream sequence following the stop codon including the 3'-UTR region (*SI Appendix,* Fig. SI5) was synthesized and cloned into the intermediate vector pNOS-AB-M (DNA-Cloning-Service, Hamburg, Germany). The expression cassette of *Rph3* was inserted into binary vector P6oUZm via the *Sfi*I cloning site to form the p*Rph3*::*Rph3* construct.

Transformation. The construct was introduced into *Agrobacterium tumefaciens* strain AGL-1 as described by Hensel et al. [113] and transformed into immature embryos of barley cv. Golden Promise according to the procedures described by Hensel et al. [114]. Selected plants were transferred to soil, and the presence of the *Rph3* gene in each plant was confirmed by PCR using specific marker MLOC_400 (forward: 5'-ACGTGAATGAAATCCGGTTC-3' and reverse: 5'-GTGCTGCTCTCCGTTGTGT-3') (*SI Appendix,* Fig. SI5, *SI Appendix*, Table S5).

Genetic diversity at the *Rph3* locus

Haplotype analysis. The genomic region covering 8.5 kb of the *Rph3* locus was divided into fragments of 5,465 and 4,882 bp with 1,428 bp overlapped for amplification. These fragments were amplified using primer pairs (5 kb_C2 and 5 kb_C5) (*SI Appendix,* Table S11), employing LongAmp® *Taq* DNA polymerase (New England BioLabs, USA) and MyFi™ DNA polymerase (Bioline, Australia) respectively, in a T100 Thermal Cycler (Bio-Rad). To amplify the 5,465 bp DNA fragment, each 10 µl PCR contained 0.1 units of LongAmp *Taq* DNA polymerase, 0.4 µM of each primer, 1x LongAmp *Taq* reaction buffer, 10 µM of each dNTP, and 50 ng of genomic DNA. The PCR was run with the block preheated to 94 °C before thermocycling. The thermocycling conditions were an initial denaturation of 95 °C for 5 minutes followed by 30 cycles of 94 °C for 30 seconds, 60 °C for 30 seconds, 65 °C for 6 minutes, and a final extension at 65 °C for 10 minutes. The components and thermocycling conditions to

amplify 4,882 bp were the same as described in the "DNA marker analysis" section but with the elongation step lasting for 5 minutes instead of 30 seconds. The amplicons were purified using AMPure XP magnetic beads (Beckman Coulter Life Sciences, USA). The sequencing template was subjected to Sanger sequencing using 28 internal primers (14 forward and 14 reverse primers) (*SI Appendix,* Table S11) that were designed from the reference DNA sequence of cv. Barke.

Allelic variation. The 78 barley accession core collection was challenged with *P. hordei* pathotypes, 200 P-, 5453 P+, and 5457 P+. Pathotype 5457 P+ differs from pathotype 5453 P+ only in being virulent on *Rph3* and is considered a single-step mutational derivative of the latter [115]. Alleles of *Rph3* conferring resistance and susceptibility were differentiated using the co-dominant cleaved amplified polymorphic sequence (CAPS) marker MLOC_198 that was completely linked to *Rph3* in the high-resolution map (*SI Appendix*, Table S12). The dominant marker Rph3_full covering the full-length sequence of *Rph3* (all exons and introns) was used to detect the presence/absence of the *Rph3* segment in these accessions. A total of 41 barley accessions postulated to carry different alleles of *Rph3* based on infection type array were subjected to Sanger sequencing of the 8,519 bp interval as described in the previous section. The sequences were aligned using the MUSCLE function at (https://www.ebi.ac.uk/Tools/msa/muscle/) to find any variation.

The frequency of *Rph3* in a diverse barley collection. Genotype-by-sequencing (GBS) was previously applied to a diverse collection of elite, landrace, and wild barley accessions (n = 22,942) by digesting genomic DNA using *Pst*I and *Msp*I endonucleases and sequenced using an Illumina HiSeq2500 [58,59]. GBS sequencing data was downloaded from NCBI for 22,628 barley accessions (PRJEB8290, PRJEB23967, PRJEB24563, PRJEB24627, and PRJEB26634). Raw GBS sequencing data for the Wild Barley Diversity Collection (n = 314) from Sallam et al. 2017 [59] was provided by Prof. Brian Steffenson (University of Minnesota). Sequencing data from cvs. Morex and Barke were initially mapped using BBmap (v38.86) to identify regions encompassing GBS markers with parameters of a minimum identity of 95% and maximum InDel of 5 bp. Two adjacent GBS markers (gRph3_I1E2 and gRph3_E2I2) mapped to the region encompassing intron 1, exon 2, and intron 2 of *Rph3*. Genomic regions with GBS markers were used as a template for *k*-mer analysis using *sect* in the *k*-mer analysis toolkit (KAT; https://github.com/TGAC/KAT) with *k*=27 [116]. For every accession, the number of non-zero *k*-mers was used as a metric for the presence or absence of the *Rph3* haplotype based on the cv. Barke genomic sequence. A bimodal distribution was identified among sequenced accessions, and a threshold of 158 *k*-mers was used to classify for the presence or absence of the *Rph3* allele. A dominant PCR marker for *Rph3* (forward: ACGTGAATGAAATCCGGTTC; reverse: GTGCTGCTCTCCGTTGTGT) was used in multiplex with primers on a BAC end sequence (0206D11_T7) from the *Mla* locus that amplified universally (forward: CTGGTTTGTTGTTGCTATGCGTTG; reverse: TCATTTGGTGTGGGGCAAAG) [117]. PCR was performed using GoTaq DNA Polymerase (Promega) in 25 µl reactions following the manufacturers' protocol. The thermocycling

conditions consisted of initial denaturation of 95 °C for 2 minutes followed by 35 cycles of 94 °C for 30 seconds, 60 °C for 30 seconds, 72 °C for 35 seconds, and a final extension at 72 °C for 5 minutes.

Prediction of RPH3 protein structure

Sequence annotation. The *Rph3* allele was extracted from the 8.5 kb DNA sequence delimited by markers MLOC_190 and MLOC_389 in cv. Barke genome. The 8.5 kb region without any annotated genes or repetitive elements was processed by the gene structure prediction program FGENESH (http://www.softberry.com/berry.phtml) using the monocotyledonous plant codon usage matrix [118] as a reference.

Prediction of secondary protein structure. After confirming the full-length cDNA using RNA-Seq data, the putative amino acid sequence of RPH3 protein was used in homology search against the Conserved Domain Database (CDD v3.18 - 55570 PSSMs) on the NCBI website (https://www.ncbi.nlm.nih.gov/Structure/cdd/wrpsb.cgi) with a default expected value threshold of 0.01. Secondary structure prediction was performed using three independent online tools, including Protter (http://wlab.ethz.ch/protter/start), TMPRED (https://embnet.vital-it.ch/software/TMPRED_form.html), and TMHMM (http://www.cbs.dtu.dk/services/TMHMM/).

Evolution history of RPH3 in cereals. The cDNA sequence of the *Rph3* allele was used as a query in the BLASTX function on NCBI to find similar proteins. The *Rph3* coding sequence was used as a query for the BLASTN function to search for homologs and orthologs in barley (https://webblast.ipk-gatersleben.de/barley_ibsc/), oat (https://avenagenome.org/), wheat (https://urgi.versailles.inra.fr/blast/?dbgroup=wheat_iwgsc_refseq_v1_chromosomes&program=blastn), and in 24 other monocot species available in ensemble plants (https://plants.ensembl.org/Multi/Tools/Blast). The duplicated subjects were removed before phylogenetic analysis. Amino acid sequences of RPH3 and its homologs/paralogs were used as an entry in SALAD (https://salad.dna.affrc.go.jp/salad/en/) to analyze their motif composition.

Phylogenetic analysis. The phylogenetic tree was constructed by the maximum likelihood using BEAST v1.10.4. Sequences were aligned using Clustal omega in EMBL-EBI (https://www.ebi.ac.uk/Tools/msa/clustalo/) before a setting step was conducted using the software BEAUti v1.10.4. Substitution model "Blosum62" [119] was chosen by the software based on the imported sequences. Other options were selected including the "Speciation: Birth-death Process" model for Tree prior [120] as the dataset contained a mixture of within- and between-species sequences, "Uncorrelated relaxed clock" for clock type with lognormal related distribution [121], and "10,000,000" for the MCMC value. The sampling frequency was set to 1,000 to have 10,000 samples recorded. The software

TreeAnnotator v1.10.4 was used to create the consensus tree that was visualized by FigTree v1.4.4. The posterior value demonstrated the likelihood of each branch.

Gene expression and functionalization

Gene expression analysis by RT-qPCR. The first leaves of the inoculated plants from the lines used in this study were harvested at different time points with three biological replicates, flash-frozen in liquid nitrogen, and then stored at -80 °C until RNA extraction. Total RNA was extracted from the samples using TRIzol™ Reagent (Thermo Fisher Scientific Ltd) following the manufacturer's instructions. The genomic DNA was digested using DNase I (Sigma-Aldrich). RNA quality was checked on agarose 1.5% gels, and quantity was reviewed on a NanoDrop™ 1000 Spectrophotometer (Thermo Fisher Scientific Ltd). RT-qPCR was performed using Luna® Universal One-Step RT-qPCR Kit (New England Biolabs®) following instructions from the manufacturer and the CFX™ Real-Time PCR Detection System (Bio-RAD). ADP-Ribosylation Factor (*ADPRF*) was used as a reference gene, and RT-qPCR data were analyzed using the ΔΔCq method. Primer sequences for RT-qPCR are listed in *SI Appendix,* Table S17.

RNA sequencing and data analysis. One set of first leaf seedlings of cv. Bowman and BW746 was inoculated with *P. hordei* pathotype 5453 P+, and a second set was used for mock inoculation. The first leaves from both treatments were harvested at two dpi and flash-frozen in liquid nitrogen until RNA extraction. Twelve samples (two genotypes, two treatments/genotype, and three biological replications/treatment) were subjected to total RNA extraction using a Spectrum™ Plant Total RNA kit (Sigma-Aldrich) following the manufacturer's instructions. The RNA samples were initially quantified using a NanoDrop™ 1000 spectrophotometer (Thermo Fisher Scientific Ltd), degradation and potential contamination were checked on 1.5% agarose gel, and RNA integrity and quantitation were measured using an Agilent 2100 analyser. A library was prepared using the NEBNext® Ultra™ RNA Library Prep Kit. RNA sequencing was conducted using an Illumina PE150 that generated 40 million paired-end reads for each sample. Individual RNA-Seq data sets were assessed for quality using FastQC (0.11.9) [122]. Trimmomatic (v0.39) was used for trimming reads using parameters 'ILLUMINACLIP:TruSeq3-PE.fa:2:30:10 LEADING:5 TRAILING:5 SLIDINGWINDOW:4:15 MINLEN:36' [123]. Pseudoalignments using Kallisto (v0.46.0) [124] were made using the barley transcriptome (high and low confidence gene models) based on the 2017 genome annotation [125] and the transcript sequence of *Rph3*. Differential gene expression analysis was carried out using DESeq2 (1.20.0) with default parameters [126]. The false discovery rate was controlled at 5% (*q*-value of 0.05). Gene ontology analysis was performed using g:Profiler. RNAseq data has been deposited in NCBI SRA in BioProject PRJNA731362.

Heterologous expression of *Rph3*

Gene cloning. To generate Rph3^{WT}, Xa10 (AGE45112), Xa23 (AIX09985), Xa27 (AAY54165) and Bs4C (AFW98885) expression constructs, the corresponding coding sequences were synthesised and cloned with the Twist

Bioscience's clonal gene synthesis service, using codon optimization for expression in *N. benthamiana*, and removal of the *Bsa*I and *Bpi*I internal restriction sites. The coding sequences were cloned into the pTwist-Kan-High-copy vector, including two flanking *Bsa*I restriction sites for subsequent Golden Gate cloning. The resulting plasmids were used in the Golden Gate assembly with pICH85281 (*mannopine synthase* + *Ω* promoter (*Mas Ω*), Addgene no. 50272), pICSL50009 (6xHA, TSL Synbio), pICSL60008 (Arabidopsis heat shock protein terminator, HSPter, TSL Synbio), and the binary vector pICH47732 (Addgene no. 48000). The $Rph3^{L93F}$ and $Rph3^{P126L}$ mutants were generated by PCR site-directed mutagenesis using Phusion High-Fidelity DNA Polymerase (Thermo Fisher), with pTwist-Kan-High-copy::$Rph3^{WT}$ as a template. The internal primers flanking the mutation sites Rph3_L93F_fw (5'-CACAACGCATtTTAACATGAATAG), Rph3_L93F_rv (5'-CTATTCATGTTAAaATGCGTTGTG), Rph3_P126L_fw (5'-GAATGGTGATCCtTAAGGATCATTC), and Rph3_P126L_rv (5'-GAATGATCCTTAaGGATCACCATTC), along with the outermost flanking primers Rph3_fw (5'-aaGAAGACaaAATGGATGCCGGAGCTTTTG) and Rph3_rv (5'- aaGAAGACaaCGAAccTGCCAGCACTACAAC), were used to generate single PCR fragments upstream and downstream of each mutation site. The purified fragments were fused by PCR using primers Rph3_fw and Rph3_rv. The resulting full-length fragments were cloned into the pICSL01005 vector (TSL Synbio) using Golden Gate assembly. PCR amplification of the $Rph3^{E72*}$ truncated mutant was done using primers Rph3_fw and Rph3_E72*_rv (5'-aaGAAGACaaCGAAccGGAGCCCTTTGTCTGAACGG). The resulting fragment was purified and used in a Golden Gate assembly with the pICSL01005 vector (TSL synbio). These assemblies were used for subsequent Golden Gate cloning into binary vectors for transient expression in a similar assembly reaction as described for $Rph3^{WT}$. In all cases, the mutants were verified by DNA sequencing. *Escherichia coli* DH5α was used for molecular cloning experiments.

Transient gene expression and cell death assays. *N. benthamiana* plants for transient gene expression assays were grown in a growth chamber held at 22-25°C with 45-65% humidity and 16 /-8 hr light-dark cycle. Transient expression in *N. benthamiana* was performed by infiltrating leaves of four-week-old plants with *A. tumefaciens* GV3101 pMP90 carrying a binary expression plasmid containing the coding sequence of the protein of interest. Bacterial suspensions were prepared in infiltration buffer (10 mM MES, 10 mM $MgCl_2$, and 150 mM acetosyringone) and adjusted to an OD_{600} = 0.4. Leaves were harvested and imaged three days post infiltration. Each experiment was performed three times, infiltrating two leaves of 3-4 plants each time.

Author contributions: R.F.P. and M.P. conceived the project. R.F.P. provided all rust isolates and information on pathogenicities and oversaw all rust phenotyping. M.A. and H.X.D. conducted histology experiments and chitin assays by confocal microscopy. H.X.D. and M.P. constructed the genetic and high-resolution maps. N.S. and M. Mascher provided the reference sequence of the *Rph3* locus, M.P. and M. Mascher annotated the final locus of *Rph3*. H.X.D. and M.P. created mutant materials, X.H.D and D.S. screened the knock-out mutants. H.X.D., D.S., R.F.P., and M.P. designed and performed the haplotype analysis. H.X.D., R.F.P. and D.S. performed a multi-pathotype test and gene postulation. H.X.D. and M.P. performed the expression analysis using RT-qPCR. M.P.

and M. Moscou designed the RNA-Seq experiment, H.X.D. experimented, M. Moscou analyzed data. H.X.D. and M.P. performed phylogenetic analysis. M.P designed the transgenic construct, G.H. created the transgenic material, and D. P. tested transgenic progeny using I-16 isolate. M. Moscou and D.G. designed and performed transient expression analysis. M. Moscou analyzed the origin and frequency of the *Rph3* allele in the barley gene bank. M.P. and R.F.P. supervised the project. H.X.D. and M.P. wrote the manuscript. All authors reviewed and commented on the manuscript.

References

1 Strange, R. N. & Scott, P. R. Plant disease: a threat to global food security. *Annual review of phytopathology* **43**, 83 (2005).

2 Savary, S. *et al.* The global burden of pathogens and pests on major food crops. *Nature ecology & evolution* **3**, 430-439 (2019).

3 Leach, J., Vera Cruz, C., Bai, J. & Leung, H. Pathogen fitness penalty as a predictor of durability of disease resistance genes. *Annual Review of Phytopathology* **39**, 187 (2001).

4 Aktar-Uz-Zaman, M., Tuhina-Khatun, M., Hanafi, M. M. & Sahebi, M. Genetic analysis of rust resistance genes in global wheat cultivars: an overview. *Biotechnology & Biotechnological Equipment* **31**, 431-445 (2017).

5 Dinh, H. X., Singh, D., Periyannan, S., Park, R. F. & Pourkheirandish, M. Molecular genetics of leaf rust resistance in wheat and barley. *Theoretical and Applied Genetics*, 1-16 (2020).

6 Lu, X. *et al.* Allelic barley MLA immune receptors recognize sequence-unrelated avirulence effectors of the powdery mildew pathogen. *Proceedings of the National Academy of Sciences of the United States of America* **113**, E6486-E6495 (2016).

7 Park, R. F. *et al.* Leaf Rust of Cultivated Barley: Pathology and Control. *Annual Review of Phytopathology* **53**, 565-589, doi:10.1146/annurev-phyto-080614-120324 (2015).

8 Mago, R. *et al.* The wheat *Sr50* gene reveals rich diversity at a cereal disease resistance locus. *Nature plants* **1**, 1-3 (2015).

9 Cloutier, S. *et al.* Leaf rust resistance gene *Lr1*, isolated from bread wheat (*Triticum aestivum* L.) is a member of the large psr567 gene family. *Plant molecular biology* **65**, 93-106 (2007).

10 Dracatos, P. M. *et al.* The coiled-coil NLR *Rph1*, confers leaf rust resistance in barley cultivar Sudan. *Plant physiology* **179**, 1362, doi:10.1104/pp.18.01052 (2019).

11 Feuillet, C. *et al.* Map-based isolation of the leaf rust disease resistance gene Lr10 from the hexaploid wheat (Triticum aestivum L.) genome. *Proceedings of the National Academy of Sciences* **100**, 15253-15258 (2003).

12 Huang, L. *et al.* Map-based cloning of leaf rust resistance gene *Lr21* from the large and polyploid genome of bread wheat. *Genetics* **164**, 655-664 (2003).

13 Thind, A. K. *et al.* Rapid cloning of genes in hexaploid wheat using cultivar-specific long-range chromosome assembly. *Nature biotechnology* **35**, 793 (2017).

14 Chen, C. *et al.* Ancient BED-domain-containing immune receptor from wild barley confers widely effective resistance to leaf rust. *bioRxiv* (2020).

15 Kolodziej, M. C. *et al.* A membrane-bound ankyrin repeat protein confers race-specific leaf rust disease resistance in wheat. *Nature communications* **12**, 1-12 (2021).

16 Krattinger, S. G. *et al.* A putative ABC transporter confers durable resistance to multiple fungal pathogens in wheat. *Science (New York, N.Y.)* **323**, 1360, doi:10.1126/science.1166453 (2009).

17 Moore, J. W. *et al.* A recently evolved hexose transporter variant confers resistance to multiple pathogens in wheat. *Nature genetics* **47**, 1494-1498 (2015).

18 Wang, Y. *et al.* Orthologous receptor kinases quantitatively affect the host status of barley to leaf rust fungi. *Nature Plants* **5**, 1129-1135, doi:10.1038/s41477-019-0545-2 (2019).

19 Kavanagh, P. J., Singh, D., Bansal, U. K. & Park, R. F. Inheritance and characterization of the new and rare gene *Rph25* conferring seedling resistance in *Hordeum vulgare* against *Puccinia hordei*. *Plant Breeding* **136**, 908-912, doi:10.1111/pbr.12535 (2017).

20 Rothwell, C. T., Singh, D., Dracatos, P. M. & Park, R. F. Inheritance and Characterization of *Rph27*: A Third Race-Specific Resistance Gene in the Barley Cultivar Quinn. *Phytopathology*, PHYTO12190470R, doi:10.1094/PHYTO-12-19-0470-R (2020).

21 Yu, X. *et al.* Genetic mapping of a barley leaf rust resistance gene *Rph26* introgressed from *Hordeum bulbosum*. *Theoretical and applied genetics* **131**, 2567, doi:10.1007/s00122-018-3173-8 (2018).

22 Roane, C. & Starling, T. Inheritance of reaction to *Puccinia hordei* in barley. II. Gene symbols for loci in differential cultivars. *Phytopathology* **57**, 66-68 (1967).

23 Jin, Y., Statler, G., Franckowiak, J. & Steffenson, B. Linkage between leaf rust resistance genes and morphological markers in barley. *Phytopathology* **83**, 230-233, doi:10.1094/Phyto-83-230 (1993).

24 Clifford, B. in *Diseases, Distribution, Epidemiology, and Control* (eds Alan P. Roelfs & William R. Bushnell) 173-205 (Academic Press, 1985).

25 Cromey, M. & Viljanen-Rollinson, S. Virulence of *Puccinia hordei* on barley in New Zealand from 1990 to 1993. *New Zealand journal of crop and horticultural science* **23**, 115-119 (1995).

26 Brooks, W. S., Griffey, C. A., Steffenson, B. J. & Vivar, H. E. Genes Governing Resistance to *Puccinia hordei* in Thirteen Spring Barley Accessions. *Phytopathology* **90**, 1131-1136, doi:10.1094/PHYTO.2000.90.10.1131 (2000).

27 Park, R. F. Annual Report: 2009–2010 Cereal Rust Survey. *The University of Sydney, Plant Breeding Institute*, 1-12 (2010).

28 Irieda, H. *et al.* Conserved fungal effector suppresses PAMP-triggered immunity by targeting plant immune kinases.(AGRICULTURAL SCIENCES)(pathogen-associated molecular pattern)(Report). *Proceedings of the National Academy of Sciences of the United States* **116**, 496, doi:10.1073/pnas.1807297116 (2019).

29 Monaghan, J. & Zipfel, C. Plant pattern recognition receptor complexes at the plasma membrane. *Current Opinion in Plant Biology* **15**, 349-357, doi:10.1016/j.pbi.2012.05.006 (2012).

30 Wilmanski, J. M., Petnicki-Ocwieja, T. & Kobayashi, K. S. NLR proteins: integral members of innate immunity and mediators of inflammatory diseases. *Journal of leukocyte biology* **83**, 13-30 (2008).

31 Toruño, T. Y., Stergiopoulos, I. & Coaker, G. Plant-pathogen effectors: cellular probes interfering with plant defenses in spatial and temporal manners. *Annual review of phytopathology* **54**, 419-441 (2016).

32 Zipfel, C. Plant pattern-recognition receptors. *Trends in Immunology* **35**, 345-351, doi:10.1016/j.it.2014.05.004 (2014).

33 Dodds, P. N. & Rathjen, J. P. Plant immunity: towards an integrated view of plant–pathogen interactions. *Nature Reviews Genetics* **11**, 539-548 (2010).

34 Padmanabhan, M., Cournoyer, P. & Dinesh-Kumar, S. P. Vol. 11 191-198 (Blackwell Publishing Ltd, Oxford, UK, 2009).

35 Mackey, D., Holt, B. F., Wiig, A. & Dangl, J. L. RIN4 Interacts with *Pseudomonas syringae* Type III Effector Molecules and Is Required for RPM1-Mediated Resistance in *Arabidopsis*. *Cell* **108**, 743-754, doi:10.1016/S0092-8674(02)00661-X (2002).

36 Axtell, M. J., Chisholm, S. T., Dahlbeck, D. & Staskawicz, B. J. Genetic and molecular evidence that the *Pseudomonas syringae* type III effector protein AvrRpt2 is a cysteine protease. *Molecular Microbiology* **49**, 1537-1546, doi:10.1046/j.1365-2958.2003.03666.x (2003).

37 Andersson, M. X., Kourtchenko, O., Dangl, J. L., Mackey, D. & Ellerström, M. Phospholipase-dependent signalling during the AvrRpm1- and AvrRpt2-induced disease resistance responses in *Arabidopsis thaliana*. *Plant Journal* **47**, 947-959, doi:10.1111/j.1365-313X.2006.02844.x (2006).

38 Kourelis, J. & van der Hoorn, R. A. L. Defended to the Nines: 25 Years of Resistance Gene Cloning Identifies Nine Mechanisms for R Protein Function. *The Plant Cell* **30**, 285-299, doi:10.1105/tpc.17.00579 (2018).

39 Martin, M. J. *et al.* Development of barley introgression lines carrying the leaf rust resistance genes *Rph1* to *Rph15*. *Crop Science* **60**, 282-302 (2020).

40 Ziems, L. *et al.* Association mapping of resistance to *Puccinia hordei* in Australian barley breeding germplasm. *Theoretical applied genetics* **127**, 1199-1212 (2014).

41 Jayakodi, M. *et al.* The barley pan-genome reveals the hidden legacy of mutation breeding. *Nature (London)* **588**, 284-289, doi:10.1038/s41586-020-2947-8 (2020).

42 Monat, C. *et al.* TRITEX: chromosome-scale sequence assembly of Triticeae genomes with open-source tools. *Genome biology* **20**, 284 (2019).

43 Devos, K. M. Updating the 'crop circle'. *Current opinion in plant biology* **8**, 155-162 (2005).

44 Lu, H. & Faris, J. D. Macro-and microcolinearity between the genomic region of wheat chromosome 5B containing the Tsn1 gene and the rice genome. *Functional & integrative genomics* **6**, 90-103 (2006).

45 Pourkheirandish, M., Wicker, T., Stein, N., Fujimura, T. & Komatsuda, T. Analysis of the barley chromosome 2 region containing the six-rowed spike gene vrs1 reveals a breakdown of rice–barley micro collinearity by a transposition. *Theoretical and applied genetics* **114**, 1357-1365 (2007).

46 Danilova, T. V., Poland, J. & Friebe, B. Production of a complete set of wheat–barley group-7 chromosome recombinants with increased grain β-glucan content. *Theoretical and Applied Genetics* **132**, 3129-3141 (2019).

47 McIntosh, R., Hart, G., Devos, K., Gale, M. & Rogers, W. in *Proc. 4th Int. Wheat Genet. Symp.* 893-937.

48 Herrera-Foessel, S. A. *et al. Lr68*: a new gene conferring slow rusting resistance to leaf rust in wheat. *Theoretical and Applied Genetics* **124**, 1475-1486 (2012).

49 Tyrka, M. a. & Chelkowski, J. Enhancing the resistance of triticale by using genes from wheat and rye. *Journal of Applied Genetics* **45**, 283-296 (2004).

50 Herrera-Foessel, S., Huerta-Espino, J., Calvo-Salazar, V., Lan, C. & Singh, R. *Lr72* confers resistance to leaf rust in durum wheat cultivar Atil C2000. *Plant Disease* **98**, 631-635 (2014).

51 Römer, P. *et al.* Plant pathogen recognition mediated by promoter activation of the pepper *Bs3* resistance gene. *Science* **318**, 645-648 (2007).

52 Tian, D. *et al*. The rice TAL effector–dependent resistance protein XA10 triggers cell death and calcium depletion in the endoplasmic reticulum. *The Plant Cell* **26**, 497-515 (2014).

53 Wang, C. *et al.* XA23 is an executor R protein and confers broad-spectrum disease resistance in rice. *Molecular plant* **8**, 290-302 (2015).

54 Keyu, G. *et al.* R gene expression induced by a type-III effector triggers disease resistance in rice. *Nature* **435**, 1122, doi:10.1038/nature03630 (2005).

55 Strauss, T. *et al.* RNA-seq pinpoints a Xanthomonas TAL-effector activated resistance gene in a large-crop genome. *Proceedings of the National Academy of Sciences of the United States of America* **109**, 19480-19485, doi:10.1073/pnas.1212415109 (2012).

56 Xu, W. *et al.* Genome Assembly of the Canadian two-row Malting Barley cultivar AAC Synergy. *G3 (Bethesda, Md.)*, doi:10.1093/g3journal/jkab031 (2021).

57 Franckowiak, J., Jin, Y. & Steffenson, B. Recommended allele symbols for leaf rust resistance genes in barley. *Barley genetics newsletter*, 36-44 (1997).

58 Milner, S. G. *et al.* Genebank genomics highlights the diversity of a global barley collection. *Nature genetics* **51**, 319-326, doi:10.1038/s41588-018-0266-x (2018).

59 Sallam, A. H. *et al.* Genome-Wide Association Mapping of Stem Rust Resistance in *Hordeum vulgare* subsp. *spontaneum*. *G3 (Bethesda, Md.)* **7**, 3491-3507, doi:10.1534/g3.117.300222 (2017).

60 Jiang, C. *et al.* Identification and Expression Pattern Analysis of Bacterial Blight Resistance Genes in *Oryza officinalis* Wall ex Watt Under *Xanthomonas oryzae* Pv. *oryzae* Stress. *Plant Molecular Biology Reporter* **37**, 436-449 (2019).

61 Xu, L. *et al.* Constitutive overexpression of cytochrome P450 monooxygenase genes contributes to chlorantraniliprole resistance in *Chilo suppressalis* (Walker). *Pest Management Science* **75**, 718, doi:10.1002/ps.5171 (2019).

62 Wen, Z. *et al.* Constitutive heterologous overexpression of a TIR-NB-ARC-LRR gene encoding a putative disease resistance protein from wild Chinese Vitis pseudoreticulata in Arabidopsis and tobacco enhances resistance to phytopathogenic fungi and bacteria. *Plant Physiology and Biochemistry* **112**, 346-361 (2017).

63 Tatis, P. A. D. *et al.* The overexpression of RXam1, a cassava gene coding for an RLK, confers disease resistance to Xanthomonas axonopodis pv. manihotis. *Planta* **247**, 1031-1042 (2018).

64 Cao, Y. *et al.* The expression pattern of a rice disease resistance gene *Xa3/Xa26* is differentially regulated by the genetic backgrounds and developmental stages that influence its function. *Genetics* **177**, 523-533 (2007).

65 Nazar, R., Castroverde, C., Xu, X., Kurosky, A. & Robb, J. Wounding induces tomato Ve1 R-gene expression. *Planta* **249**, 1779-1797, doi:10.1007/s00425-019-03121-6 (2019).

66 Domingo, C., Andrés, F., Tharreau, D., Iglesias, D. J. & Talón, M. Constitutive expression of OsGH3. 1 reduces auxin content and enhances defense response and resistance to a fungal pathogen in rice. *Molecular plant-microbe interactions* **22**, 201-210 (2009).

67 Zhang, Z. *et al*. Constitutive expression of a novel antimicrobial protein, Hcm1, confers resistance to both Verticillium and Fusarium wilts in cotton. *Scientific reports* **6**, 1-13 (2016).

68 Ali, S. *et al.* Overexpression of NPR1 in Brassica juncea confers broad spectrum resistance to fungal pathogens. *Frontiers in plant science* **8**, 1693 (2017).

69 Yoshimura, S. *et al.* Expression of *Xa1*, a bacterial blight-resistance gene in rice, is induced by bacterial inoculation. *Proceedings of the National Academy of Sciences, USA* **95**, 1663-1668 (1998).

70 Zhang, J., Yin, Z. & White, F. TAL effectors and the executor R genes. *Frontiers in plant science* **6**, 641 (2015).

71 Levy, M., Edelbaum, O. & Sela, I. Tobacco mosaic virus regulates the expression of its own resistance gene N. *Plant physiology* **135**, 2392-2397 (2004).

72 Caldo, R. A., Nettleton, D. & Wise, R. P. Interaction-dependent gene expression in *Mla*-specified response to barley powdery mildew. *The Plant Cell* **16**, 2514-2528 (2004).

73 Radwan, O., Mouzeyar, S., Nicolas, P. & Bouzidi, M. F. Induction of a sunflower CC-NBS-LRR resistance gene analogue during incompatible interaction with Plasmopara halstedii. *Journal of Experimental Botany* **56**, 567-575, doi:10.1093/jxb/eri030 (2004).

74 Rai, A. *et al.* Functional complementation of rice blast resistance gene *Pi-k*^{h} (*Pi54*) conferring resistance to diverse strains of *Magnaporthe oryzae*. *Journal of Plant Biochemistry and Biotechnology* **20**, 55-65, doi:10.1007/s13562-010-0026-1 (2011).
75 Wang, J. *et al.* The pepper Bs4C proteins are localized to the endoplasmic reticulum (ER) membrane and confer disease resistance to bacterial blight in transgenic rice. *Molecular plant pathology* **19**, 2025-2035 (2018).
76 Krönauer, C., Kilian, J., Strauß, T., Stahl, M. & Lahaye, T. Cell Death Triggered by the YUCCA-like Bs3 Protein Coincides with Accumulation of Salicylic Acid and Pipecolic Acid But Not of Indole-3-Acetic Acid. *Plant physiology* **180**, 1647-1659 (2019).
77 van der Hoorn, R. A. & Kamoun, S. From guard to decoy: a new model for perception of plant pathogen effectors. *The Plant Cell* **20**, 2009-2017 (2008).
78 Kay, S., Hahn, S., Marois, E., Hause, G. & Bonas, U. A bacterial effector acts as a plant transcription factor and induces a cell size regulator. *Science* **318**, 648-651 (2007).
79 Krattinger, S. G. & Keller, B. Trapping the intruder—immune receptor domain fusions provide new molecular leads for improving disease resistance in plants. *Genome biology* **17**, 23 (2016).
80 Chen, S. *et al.* Wheat gene Sr60 encodes a protein with two putative kinase domains that confers resistance to stem rust. *New Phytologist* **225**, 948-959 (2020).
81 Zheng, S. *et al.* Characterization and diagnostic marker development for Yr28-rga1 conferring stripe rust resistance in wheat. *European Journal of Plant Pathology* **156**, 623-634 (2020).
82 Michelmore, R. W., Christopoulou, M. & Caldwell, K. S. Impacts of resistance gene genetics, function, and evolution on a durable future. *Annual review of phytopathology* **51**, 291-319 (2013).
83 Van de Weyer, A.-L. *et al.* A species-wide inventory of NLR genes and alleles in *Arabidopsis thaliana*. *Cell* **178**, 1260-1272. e1214 (2019).
84 Brueggeman, R. *et al.* The barley stem rust-resistance gene *Rpg1* is a novel disease-resistance gene with homology to receptor kinases. *Proceedings of the National Academy of Sciences* **99**, 9328-9333 (2002).
85 Chen, X. *et al. Xa7*, a new executor R gene that confers durable and broad-spectrum resistance to bacterial blight disease in rice. *Plant Communications*, 100143, doi:10.1016/j.xplc.2021.100143 (2021).
86 Wu, L., Goh, M. L., Sreekala, C. & Yin, Z. XA27 depends on an amino-terminal signal-anchor-like sequence to localize to the apoplast for resistance to *Xanthomonas oryzae* pv *oryzae*. *Plant physiology* **148**, 1497-1509, doi:10.1104/pp.108.123356 (2008).
87 Iuchi, S. *et al.* Regulation of drought tolerance by gene manipulation of 9- cis -epoxycarotenoid dioxygenase, a key enzyme in abscisic acid biosynthesis in Arabidopsis. *Plant Journal* **27**, 325-333, doi:10.1046/j.1365-313x.2001.01096.x (2001).
88 Huang, Y. *et al.* OsNCED5, a 9-cis-epoxycarotenoid dioxygenase gene, regulates salt and water stress tolerance and leaf senescence in rice. *Plant Science* **287**, 110188 (2019).
89 Huang, Y. *et al.* 9-cis-Epoxycarotenoid dioxygenase 3 regulates plant growth and enhances multi-abiotic stress tolerance in rice. *Frontiers in plant science* **9**, 162 (2018).
90 Xie, X. *et al.* The identification of genes involved in the stomatal response to reduced atmospheric relative humidity. *Current Biology* **16**, 882-887 (2006).
91 McAdam, S. A. & Brodribb, T. J. Linking turgor with ABA biosynthesis: implications for stomatal responses to vapor pressure deficit across land plants. *Plant Physiology* **171**, 2008-2016 (2016).
92 Thompson, A. J. *et al.* Ectopic expression of a tomato 9-cis-epoxycarotenoid dioxygenase gene causes over-production of abscisic acid. *The Plant Journal* **23**, 363-374 (2000).
93 Montillet, J.-L. *et al.* An abscisic acid-independent oxylipin pathway controls stomatal closure and immune defense in Arabidopsis. *PLoS biology* **11** (2013).
94 Hernández-Blanco, C. *et al.* Impairment of cellulose synthases required for Arabidopsis secondary cell wall formation enhances disease resistance. *The Plant Cell* **19**, 890-903 (2007).
95 Linkun, L., Xusheng, H. & Huiming, Z. Expression and Response Analysis of *NCED* Gene of *Zoysia japonica* in Initial Infection Stage of *Rhizoctonia solani*. *Plant Diseases and Pests* **8**, 23-26, doi:10.19579/j.cnki.plant-d.p.2017.05.007 (2017).
96 Krattinger, S. G. *et al.* Abscisic acid is a substrate of the ABC transporter encoded by the durable wheat disease resistance gene *Lr34*. *New Phytologist* **223**, 853-866 (2019).
97 Harlan, J. R. Agricultural origins: centers and noncenters. *Science* **174**, 468-474 (1971).
98 Salamini, F., Özkan, H., Brandolini, A., Schäfer-Pregl, R. & Martin, W. Genetics and geography of wild cereal domestication in the near east. *Nature Reviews Genetics* **3**, 429-441 (2002).

99 Pourkheirandish, M. *et al.* Evolution of the Grain Dispersal System in Barley. *Cell* **162**, 527-539, doi:10.1016/j.cell.2015.07.002 (2015).

100 Doebley, J. F., Gaut, B. S. & Smith, B. D. The molecular genetics of crop domestication. *Cell* **127**, 1309-1321 (2006).

101 Pourkheirandish, M., Golicz, A. A., Bhalla, P. L. & Singh, M. B. Global role of crop genomics in the face of climate change. *Frontiers in plant science* **11**, 922-922, doi:10.3389/fpls.2020.00922 (2020).

102 Pourkheirandish, M. & Komatsuda, T. The importance of barley genetics and domestication in a global perspective. *Annals of Botany* **100**, 999-1008 (2007).

103 Pourkheirandish M., Golicz A., Bhalla P. & M., S. Global role of crop genomics in the face of climate change. *Frontiers in Plant Science* (2020).

104 Henderson, M. T. *Studies of sources of resistance and inheritance of reaction to leaf rust, Puccinia anomala Rostr., in barley*. (University of Minnesota., 1945).

105 Ayliffe, M. *et al.* Nonhost resistance of rice to rust pathogens. *Molecular Plant-Microbe Interactions* **24**, 1143-1155 (2011).

106 Ayliffe, M. *et al.* A simple method for comparing fungal biomass in infected plant tissues. *Molecular plant-microbe interactions : MPMI* **26**, 658-667, doi:10.1094/MPMI-12-12-0291-R (2013).

107 Gilmour, J. Octal notation for designating physiologic races of plant pathogens. *Nature* **242**, 620-620 (1973).

108 Park, R. Pathogenic specialization and pathotype distribution of *Puccinia hordei* in Australia, 1992 to 2001. *Plant disease* **87**, 1311-1316 (2003).

109 Stakman, E. C., Stewart, D. & Loegering, W. *Identification of physiologic races of Puccinia graminis var. tritici*. (USDA Washington, 1962).

110 Park, R. F. & Karakousis, A. Characterization and mapping of gene *Rph19* conferring resistance to *Puccinia hordei* in the cultivar 'Reka 1'and several Australian barleys. *Plant Breeding* **121**, 232-236 (2002).

111 Kumar, S., Stecher, G., Li, M., Knyaz, C. & Tamura, K. MEGA X: molecular evolutionary genetics analysis across computing platforms. *Molecular biology and evolution* **35**, 1547-1549 (2018).

112 Caldwell, D. G. *et al.* A structured mutant population for forward and reverse genetics in Barley (*Hordeum vulgare* L.). *Plant Journal* **40**, 143-150, doi:10.1111/j.1365-313X.2004.02190.x (2004).

113 Hensel, G., Valkov, V., Middlefell-Williams, J. & Kumlehn, J. Efficient generation of transgenic barley: The way forward to modulate plant–microbe interactions. *Journal of Plant Physiology* **165**, 71-82, doi:10.1016/j.jplph.2007.06.015 (2008).

114 Hensel, G., Kastner, C., Oleszczuk, S., Riechen, J. & Kumlehn, J. Agrobacterium-mediated gene transfer to cereal crop plants: current protocols for barley, wheat, triticale, and maize. *International journal of plant genomics* **2009**, 835608-835608, doi:10.1155/2009/835608 (2009).

115 Chen, J. *et al.* De novo genome assembly and comparative genomics of the barley leaf rust pathogen *Puccinia hordei* identifies candidates for three avirulence genes. *G3: Genes, Genomes, Genetics* **9**, 3263-3271 (2019).

116 Mapleson, D., Garcia Accinelli, G., Kettleborough, G., Wright, J. & Clavijo, B. J. KAT: a K-mer analysis toolkit to quality control NGS datasets and genome assemblies. *Computer applications in the biosciences* **33**, 663-576, doi:10.1093/bioinformatics/btw663 (2016).

117 Wei, F. *et al.* The Mla (Powdery Mildew) Resistance Cluster Is Associated With Three NBS-LRR Gene Families and Suppressed Recombination Within a 240-kb DNA Interval on Chromosome 5S (1HS) of Barley. *Genetics (Austin)* **153**, 1929-1948 (1999).

118 Solovyev, V., Kosarev, P., Seledsov, I. & Vorobyev, D. Automatic annotation of eukaryotic genes, pseudogenes and promoters. *Genome biology* **7**, S10 (2006).

119 Henikoff, S. & Henikoff, J. G. Amino acid substitution matrices from protein blocks. *Proceedings of the National Academy of Sciences* **89**, 10915-10919 (1992).

120 Gernhard, T. Using birth-death model on trees. *J Theor Biol* **253**, 769-778 (2008).

121 Drummond, A. J., Ho, S. Y., Phillips, M. J. & Rambaut, A. Relaxed phylogenetics and dating with confidence. *PLoS biology* **4** (2006).

122 Andrews, S. (Babraham Bioinformatics, Babraham Institute, Cambridge, United Kingdom, 2010).

123 Bolger, A. M., Lohse, M. & Usadel, B. Trimmomatic: a flexible trimmer for Illumina sequence data. *Bioinformatics* **30**, 2114-2120 (2014).

124 Bray, N. L., Pimentel, H., Melsted, P. & Pachter, L. Near-optimal probabilistic RNA-seq quantification. *Nature biotechnology* **34**, 525-527 (2016).

125 Beier, S. *et al*. Construction of a map-based reference genome sequence for barley, *Hordeum vulgare* L. *Scientific data* **4**, 170044-170044, doi:10.1038/sdata.2017.44 (2017).
126 Love, M. I., Huber, W. & Anders, S. Moderated estimation of fold change and dispersion for RNA-seq data with DESeq2. *Genome biology* **15**, 550 (2014).

FIGURES

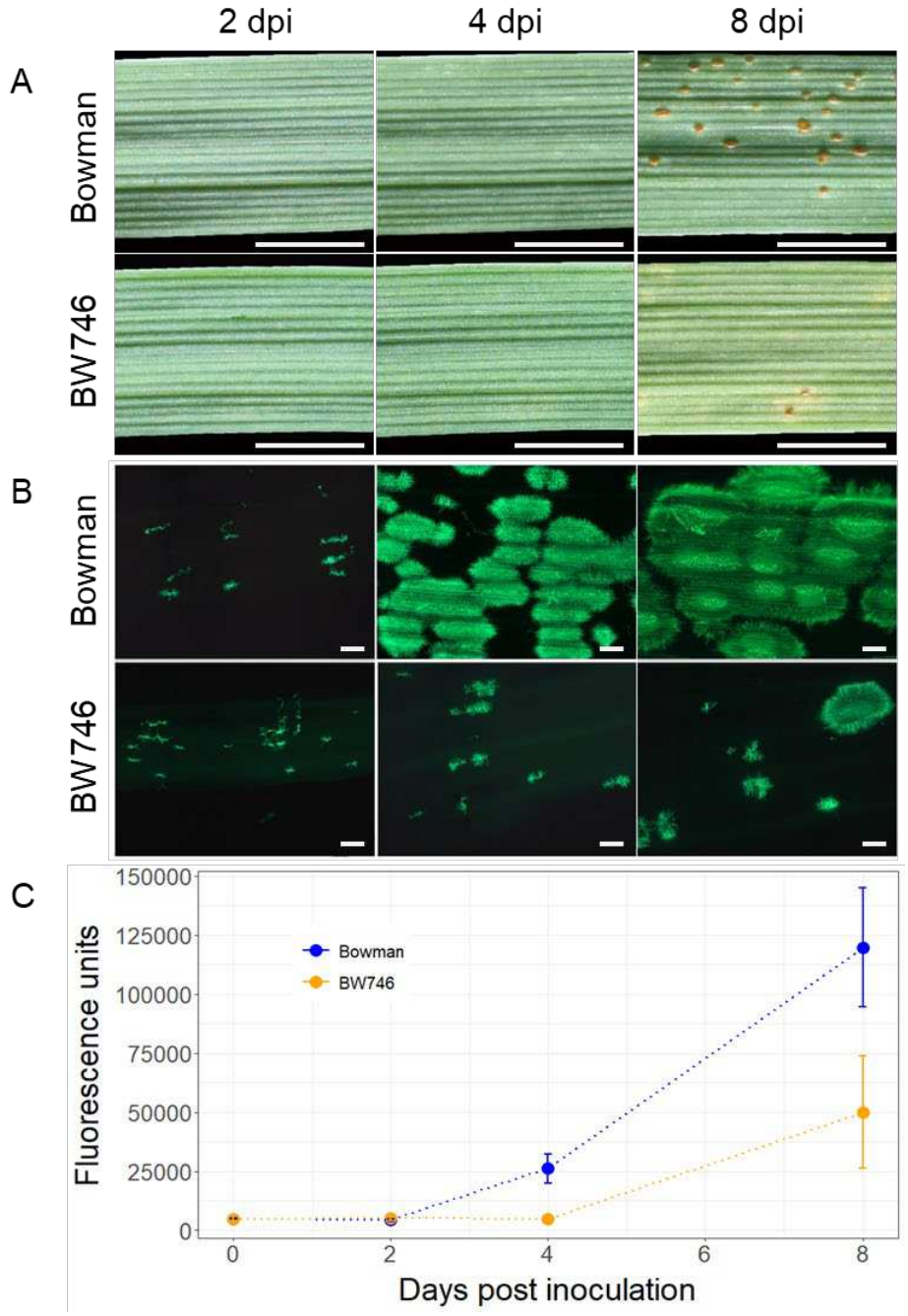

Fig. 1. Development of *Puccinia hordei* in leaves of cv. Bowman (*rph3*) compared to its near-isogenic line BW746 (*Rph3*). (*A*) Segments of infected leaves of cv. Bowman (top) and BW746 (bottom) at 2, 4, and 8 dpi. The scale bar is 0.5 cm. The photos were taken from the same leaves throughout the time points. (*B*) Microscopic visualization of WGA-FITC-stained fungal colonization of mesophyll cells of cv. Bowman and BW746 leaves at 2, 4, and 8 dpi. The scale bar is 200 µm. (*C*) Quantification of *P. hordei* growth in cv. Bowman and BW746 leaves by the wheat germ agglutinin chitin assay. Fluorescence values for cv. Bowman are shown as blue dots; those from BW746 shown as orange dots.

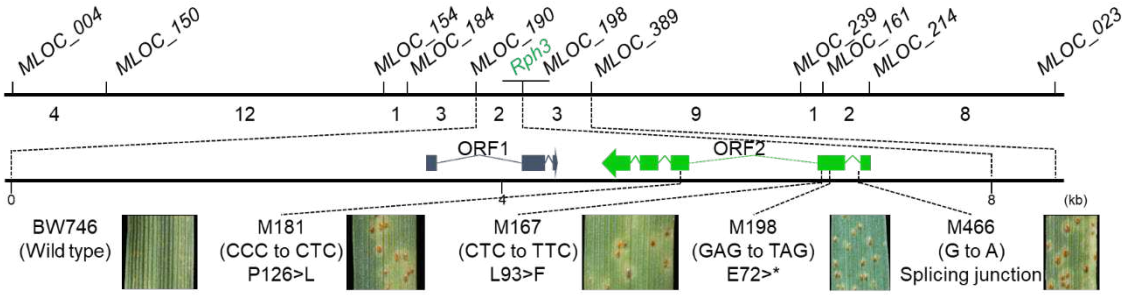

Fig. 2. Map-based cloning of barley leaf rust resistance gene *Rph3.* A high-resolution genetic linkage and physical map of the *Rph3* locus were constructed based on segregation among 10,411 F_2 individuals. Forty-five recombinants were found between flanking markers MLOC_004 and MLOC_023. The *Rph*3 gene was physically located in an 8,519 bp interval based on cv. Barke reference sequence. Two putative genes identified within the window are shown as *ORF1* and *ORF2*. Four independent EMS-induced mutants within the coding sequence of *ORF2* indicated that the *ORF2* was required for *Rph3* resistance.

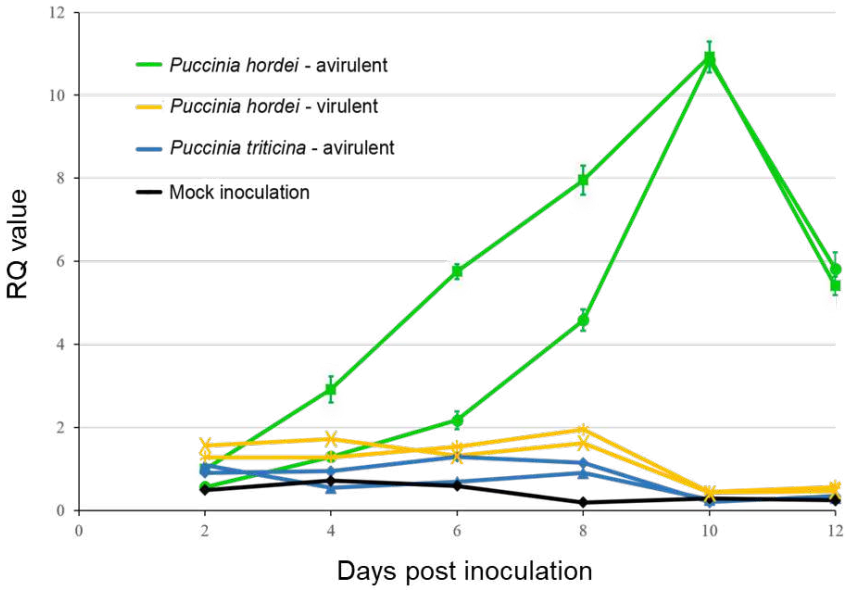

Fig. 3. Transcript levels of *Rph3* detected by RT-qPCR during 2-12 dpi in response to virulent and avirulent pathotypes. The *Rph3* gene was up-regulated when the leaf was infected by *Rph3*-avirulent *P. hordei* pathotypes (green dot = 200 P-, green square = 5453 P+), whereas the transcript levels were unchanged when the leaf was infected by *Rph3*-virulent pathotypes (yellow cross = 5656 P+, yellow asterisk = 5457 P+) and *P. triticina* (blue diamond = 26-0, blue triangle = 104-1,2,3,(6),(7),11,13). The transcript levels of *Rph3* in un-inoculated seedlings (mock inoculation) is shown in the black line. Values represent means ± SD (n=3). Samples inoculated with pathotype 5453 P+ at two dpi were used

as calibrations to calculate the relative quantification (RQ) values using the delta-delta method with $RQ = 2^{-\Delta\Delta Cq}$. The ADP-ribosylation factor gene was used as a normalizer.

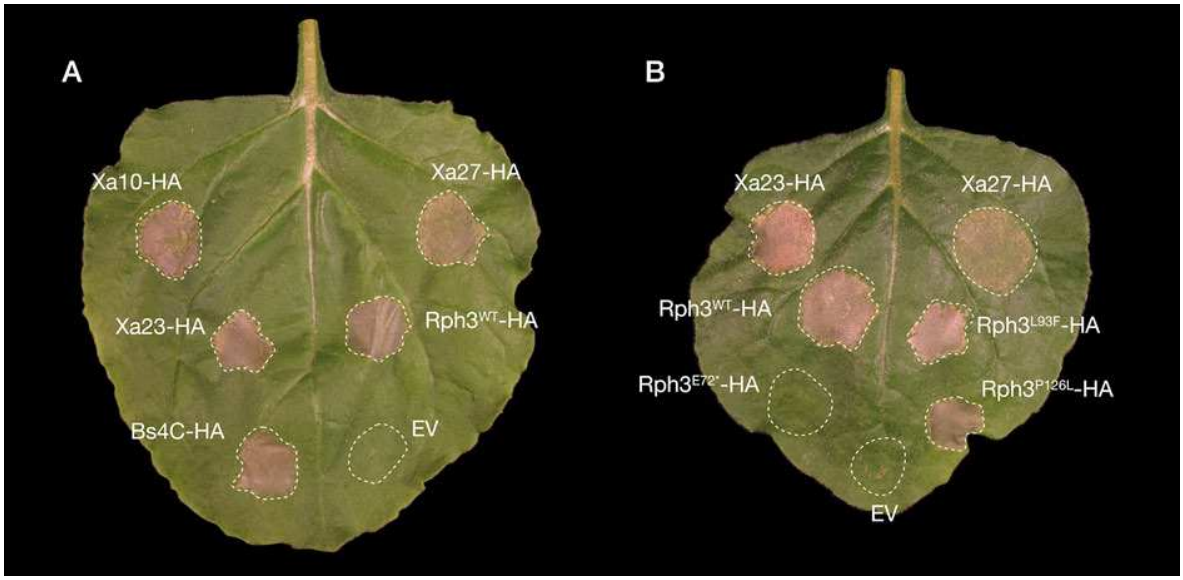

Fig. 4. *Rph3* induces cell death in *N. benthamiana.* (*A*) Transient expression of executor resistance genes (*Xa10*, *Xa27*, *Xa23* and *Bs4C*) and *Rph3* (C-terminal HA-tagged) induce cell death in *N. benthamiana* under a mas promoter. (*B*) Non-synonymous *Rph3* mutants M167 (L93F) and M181 (P126L) retained the ability to cause cell death in *N. benthamiana,* whereas the truncation mutant M198 (E72*) did not. *Xa23* and *Xa27* were used as controls for induction of cell death. The experiment was performed three times and included infiltration of two leaves of three to four plants with similar results.

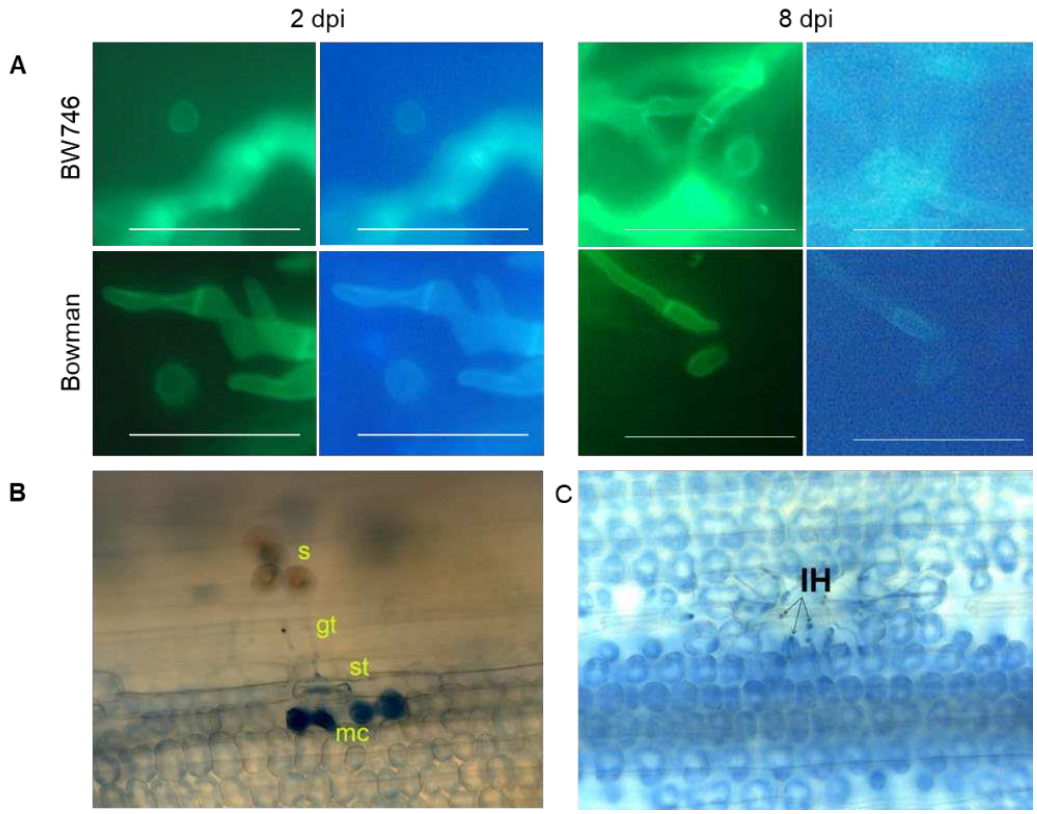

Fig. SI1. Infection of resistant and susceptible barley lines with *Puccinia hordei* pathotype 5453 P+. (*A*) At two dpi, haustoria (H), haustorial mother cells (HMC), and infection hyphae (IH) were observed in both host genotypes (left panels). At eight dpi, the infection hyphae and haustoria were more abundant in susceptible cv. Bowman compared to resistant line BW746 (left panels). Under UV light (right panels), no autofluorescence was apparent in either line. The scale bar is 20 µm. (*B*) Four mesophyll cells (mc) of BW746 in contact with a stomatal cell (st) were strongly stained with trypan blue, indicating changed membrane permeability suggestive of cell death in response to infection. Germinated spores (s) and germ tubes (gt) can be seen on the leaf surface. (*C*) All mesophyll cells of Bowman have uniform staining indicating no change in membrane structure in infected cells. The small blue dots arrowed are infection hyphae (IH).

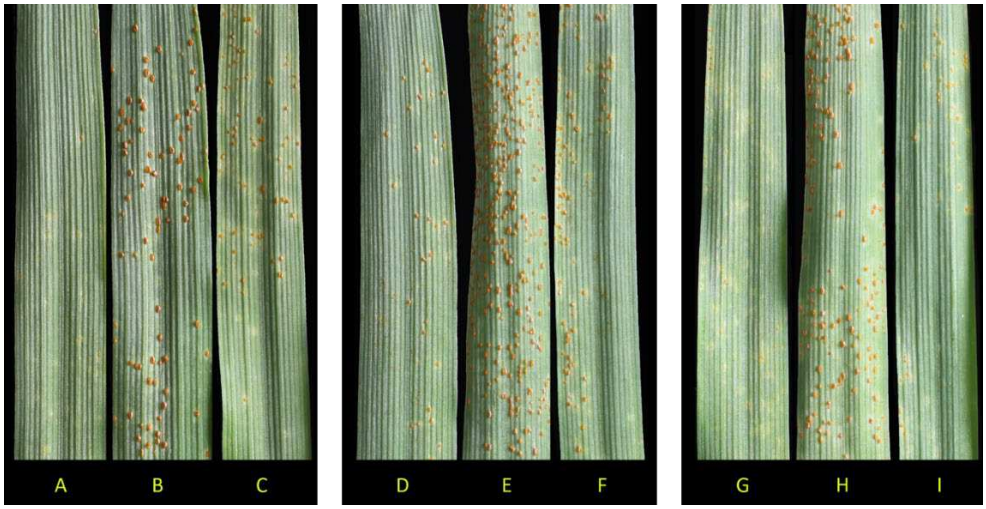

Fig. SI2. *Rph3* is incompletely dominant. Infection types observed in resistant, susceptible parents and offspring. (*A*) Scarlett (*Rph3/Rph3*); (*B*) Tallon (*rph3/rph3*); (*C*) Scarlett x Tallon F_1 (*Rph3/rph3*); (*D*) Alexis (*Rph3/Rph3*); (*E*) Sloop (*rph3/rph3*); (F) Alexis x Sloop F_1 (*Rph3/rph3*); (G) BW746 (*Rph3/Rph3*); (*H*) Bowman (*rph3/rph3*); (*I*) BW746 x Bowman F_1 (*Rph3/rph3*).

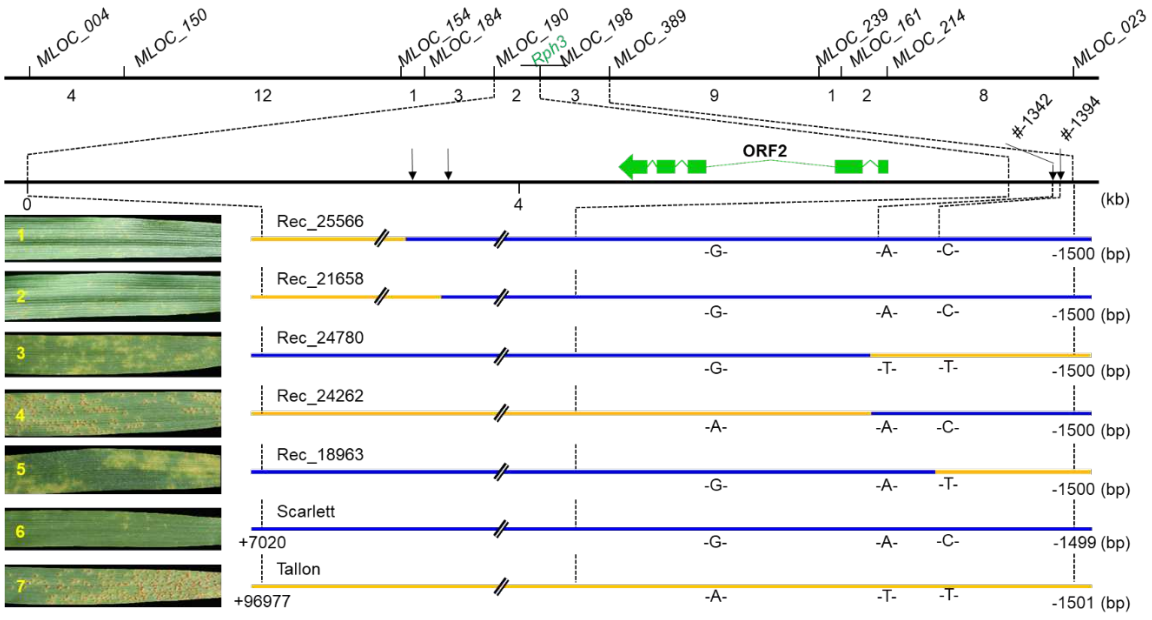

Fig. SI3. Locations of recombination events in the vicinity of the *Rph3* gene were confirmed by Sanger sequencing. The genetic and physical map of the *Rph3* locus delimited by the closest flanking markers MLOC_190 and MLOC_389. The crossover occurred between the nucleotide position -1342 and -970, resulting in genotype changes from *Rph3* (represented by blue part) to *rph3* (represented by the orange part) in the plant numbered 24262 and vice versa in the plant numbered 24780; the crossover between the nucleotide position -1342 and -1394 resulted in the genotype change from *Rph3* to *rph3* in the plant numbered 18963. The infection type observed in resistant (1), susceptible (5) parents, and three families (2, 3, 4) carrying critical recombinants upstream of *Rph3*.

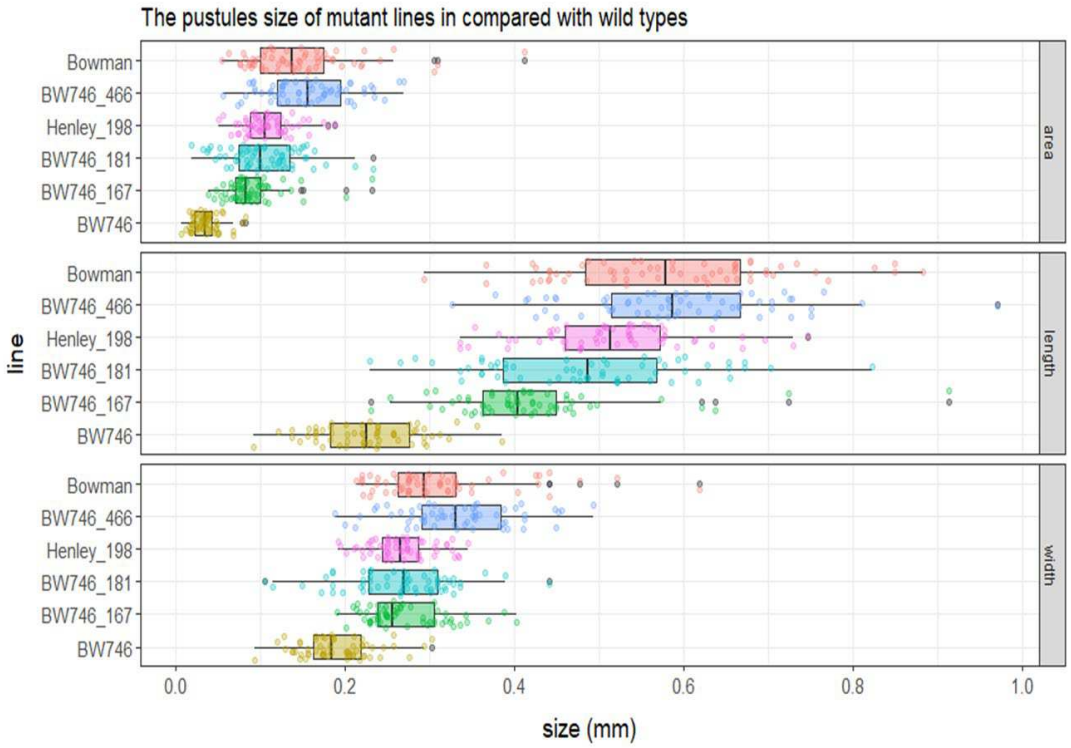

Fig. SI4. Uredinium size of *P. hordei* pathotype 5453 P+ in the knock-out mutants. The data for each mutant were gathered from 60 uredinia (3 leaves × 20 uredinia/leaf) using the ImageJ software. Each box plot shows the minimum, maximum, and median values.

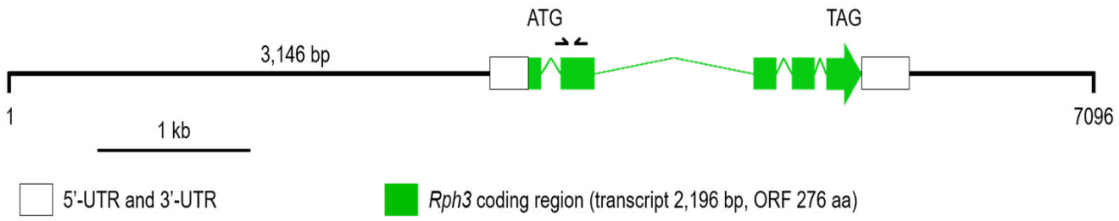

Fig. SI5. The transgene sequence comprised a 7,096 bp genomic fragment harbouring the *Rph3* coding sequence with its native promoter. Exons are shown as green squares with the arrow in the last exon showing the transcript direction. The *Rph3* gene (including introns and exons) was 2,196 bp. The 5'-UTR and 3'-UTR of 254- and 292-bp, respectively, are shown as white squares. Black arrows illustrate the position of the diagnostic MLOC_400 marker for the *Rph3* gene.

A

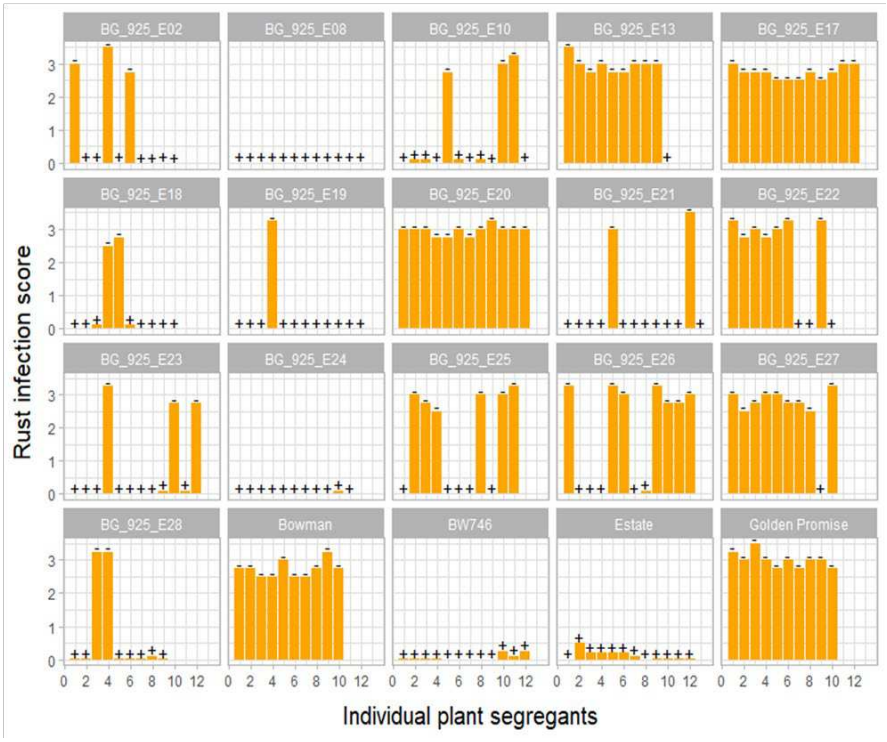

B

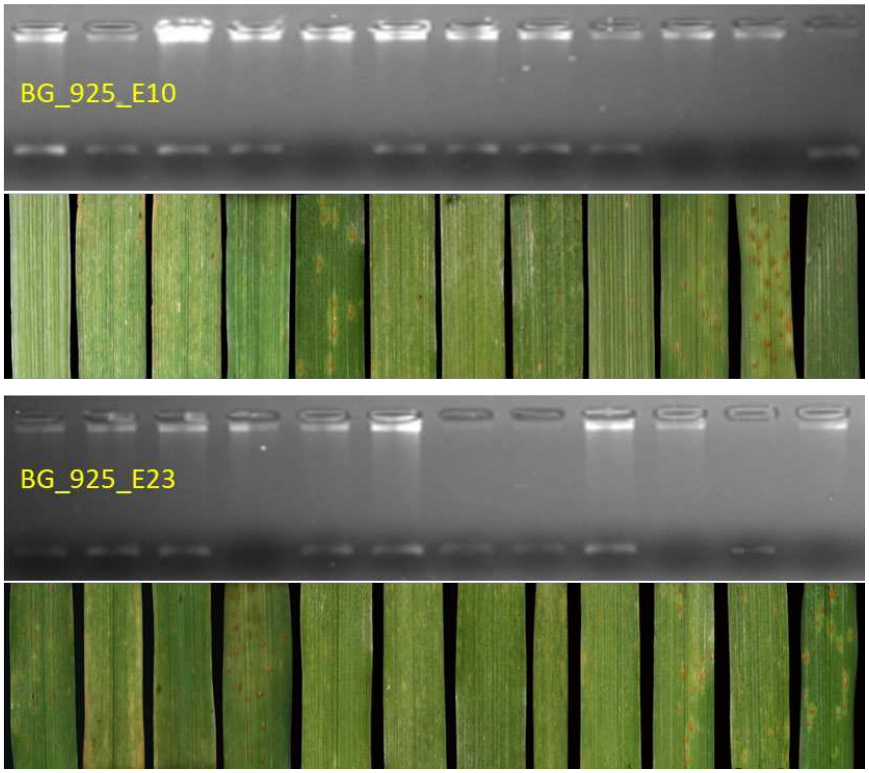

Fig. SI6. Progeny tests of *Rph3* transgenic plants. (*A*) The responses *to P. hordei* pathotype 16-3 of 16 independent transformants. The transgene plants with (+) and without (-) *Rph3* were identified by the dominant marker MLOC_400. (*B*) Phenotypes of some transgenic gene families. The bands on the agarose gel show presence of the *Rph3* marker. The image under the agarose gel shows the leaf rust response.

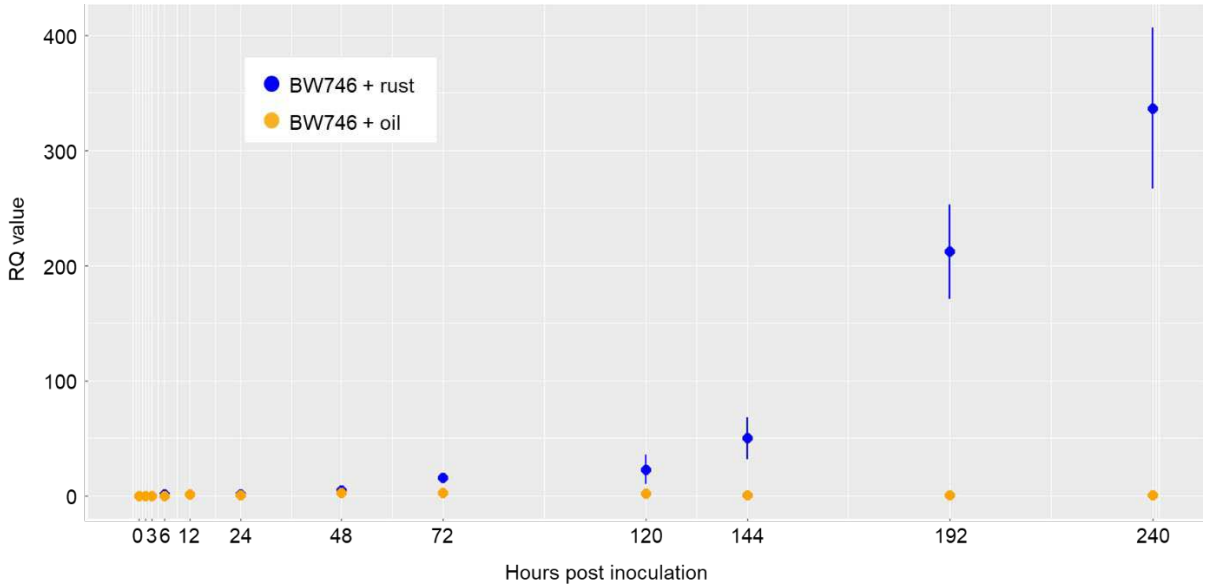

Fig. SI7. Expression profile of the *Rph3* allele in an extended time course. Blue dots indicate the expression of *Rph3* for the treatment challenged with *P. hordei* pathotype 5453 P+ and by orange dots for the mock inoculation.

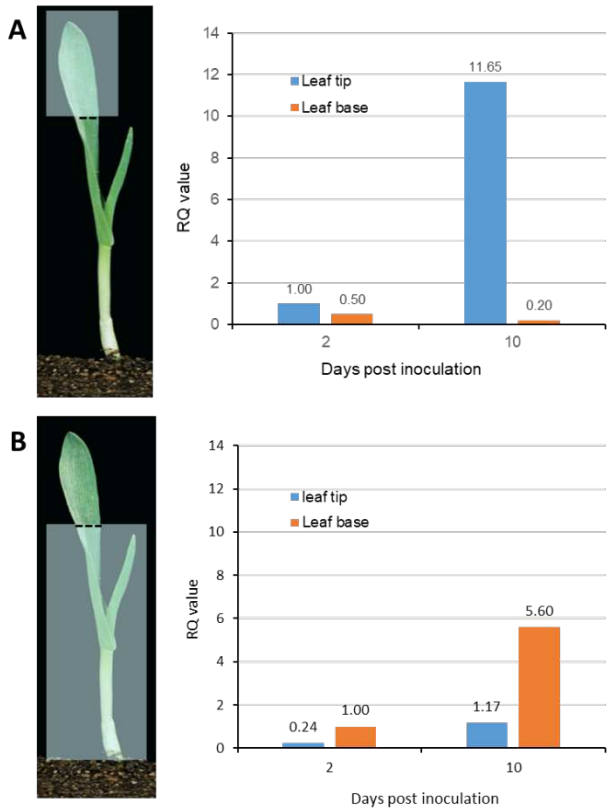

Fig. SI8. Localized expression of the *Rph3* allele in cv. BW746 challenged with *P. hordei* pathotype 5453 P+. Distal (*A*) and proximal (*B*) leaf sections were inoculated separately as illustrated, and expression in the respective host tissues was determined. Relative quantification (RQ) value was calculated using the delta-delta method with RQ = $2^{-\Delta\Delta Cq}$.

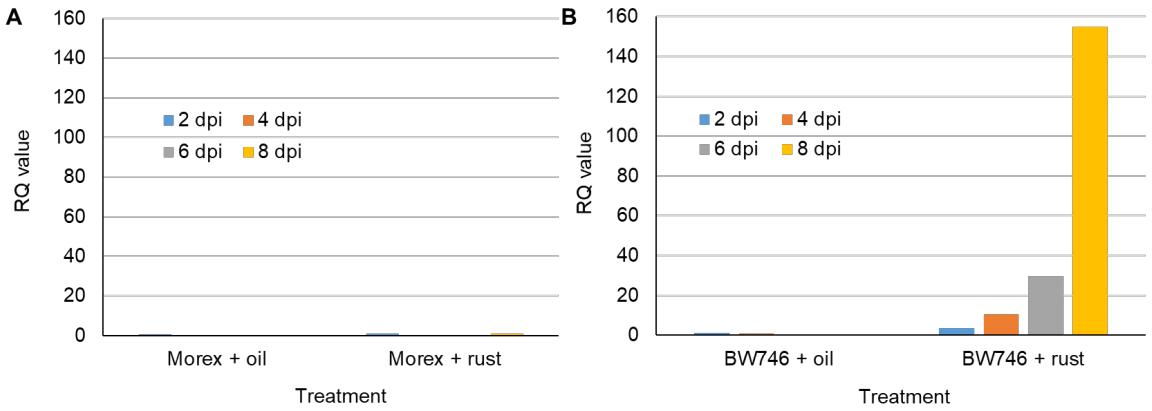

Fig. SI9. Expression profiles for susceptible (cv. Morex, *rph3*) and resistant (BW746, *Rph3*) genotypes when treated with oil alone or challenged with *P. hordei* pathotype 5453 P+. (*A*) The expression profile of homologs of the *Rph3* gene in susceptible cv. Morex. The marker was designed based on a conserved sequence among four homologs, namely *Morex_ORF5*, *Morex_ORF10*, *Morex_ORF11,* and *Morex_ORF12,* so that it can detect the transcript level of all these genes in total. (*B*) The expression profile of *Rph3* was examined by using the marker Rph3_qPCR7. The relative quantification (RQ) value was calculated using the delta-delta method with RQ = $2^{-\Delta\Delta Cq}$.

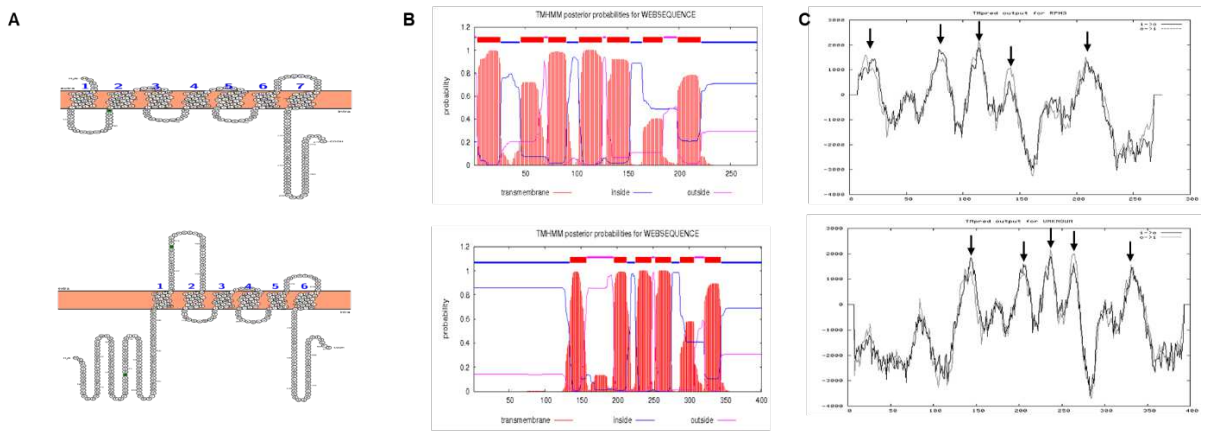

Fig. SI10. Predicted secondary structure of RPH3 protein (upper) and its ortholog in the wheat D genome (lower). (*A*) The prediction made by Protter in which RPH3 protein has seven transmembrane helices, whereas TraesCS7D_RPH3_LIKE has six transmembrane helices. N-glycol motifs are marked in green. Prediction made by the TMHMM (*B*) and TMPRED (*C*) tools; arrows indicate the transmembrane helices.

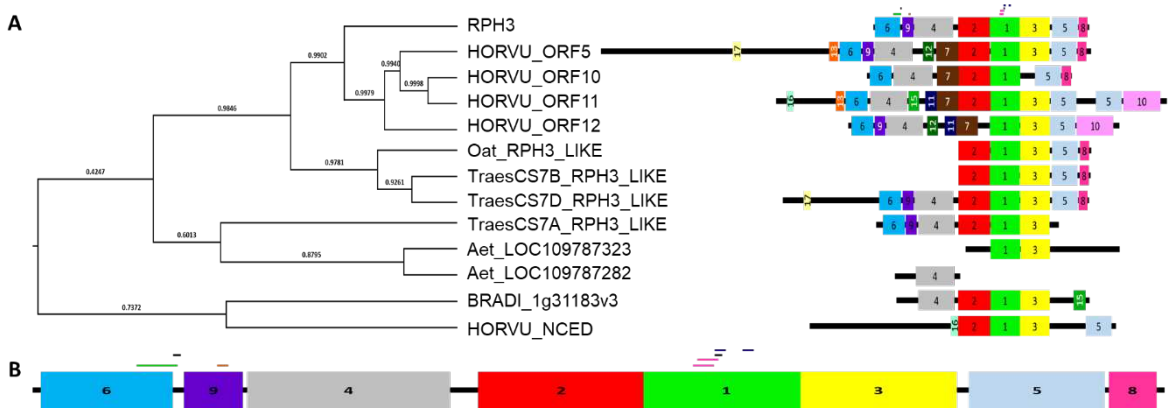

1183

1184 **Fig. SI11.** Origin of the *Rph3* allele. (*A*) Comparison of the *Rph3* sequence with *rph3* in cv. Morex and
1185 homologs in other species. Four copies of the recessive allele were found in the susceptible haplotype
1186 (cv. Morex) encoding four HORVU proteins shown in the phylogenetic tree. The homologs were also
1187 found in other crop species, including wheat A, B, and D genomes (three TraesCS proteins),
1188 *Brachypodium distachyon* (BRADI protein), and *Aegilops tauschii* (two Aet proteins). The tree was
1189 constructed using the maximum likelihood approach based on the protein sequences. The sequences
1190 were aligned using Clustal Omega before the phylogenetic analysis. (*B*) Motifs present in RPH3
1191 homologs. Five homologs of RPH3 in barley include HORVU_NCED sharing 46% identity, HORVU_ORF5
1192 with 72% identity, HORVU_ORF10 with 69% identity, HORVU_ORF11 with 90% identity, and
1193 HORVU_ORF12 with 72% identity. Three orthologs of RPH3 on wheat A, B, and D genome (named
1194 TRaesCS7A_RPH3_LIKE, TRaesCS7B_RPH3_LIKE, and TRaesCS7D_RPH3_LIKE) share 57%, 88% and 88%
1195 identity with RPH3 respectively. Two orthologs from *Aegilops tauschii* (named Aet_LOC109787323
1196 and Aet_LOC109787282) shared 41% and 42% identity with RPH3, respectively. The ortholog in
1197 *Brachypodium distachyon* (BRADI_1g31183v3) has 57% identity with RPH3 and Oat_RPH3_LIKE in oat
1198 shares 86% identity with RPH3. Motif 1 contains two N-myristoylation sites (pink bars),
1199 phosphorylation site of protein kinase C (black bar), and phosphorylation sites of casein kinase II (blue
1200 bars), motif 6 contains the serpin signature (green bar), and motif 9 contains N-glucosylation site
1201 (brown bar).

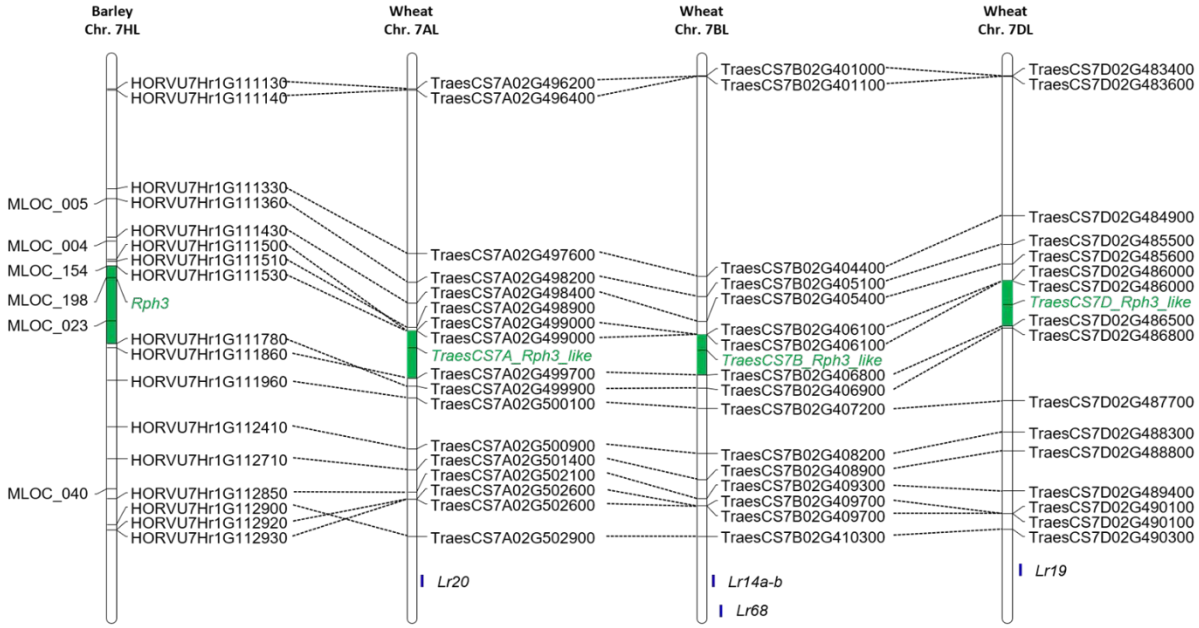

Fig. SI12. Synteny on chromosome 7HL was highly conserved in wheat. Most of the annotated high-confidence genes in barley have their homolog/orthologs in the wheat A, B, and D sub-genomes. The physical windows of the *Rph3* locus are shown as green boxes, and possible orthologs of *Rph3* are green scripts. Four designated wheat leaf rust resistance loci on the long arm of chromosomes 7A, 7B, and 7D are shown by blue bars.

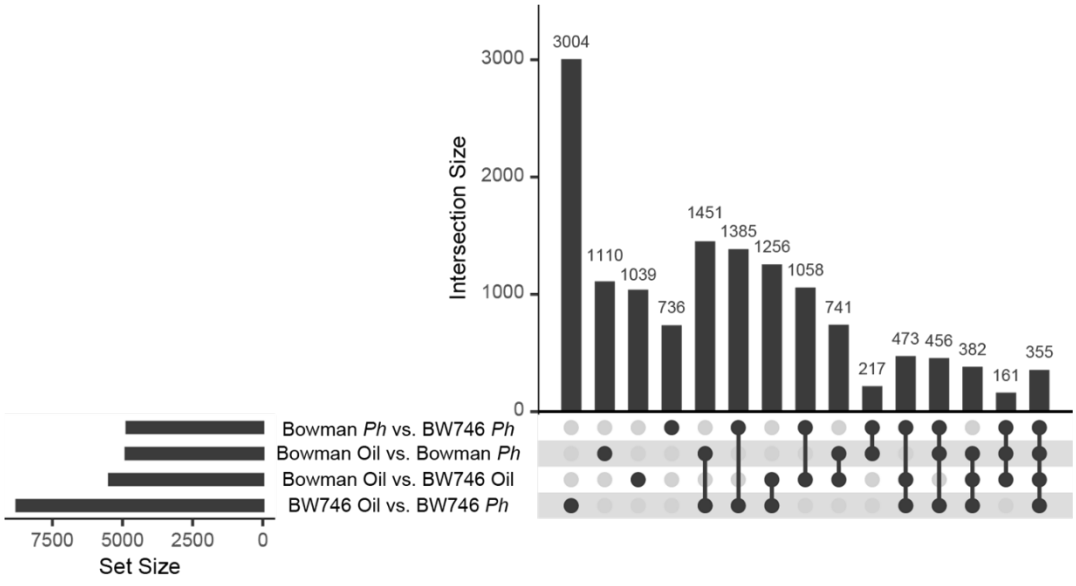

Fig. SI13. Pair-wise comparison of differentially expressed genes identified in cv. Bowman (*rph3*) and near-isogenic BW746 (*Rph3*) inoculated with *P. hordei* or oil alone (mock) at two days post-inoculation.

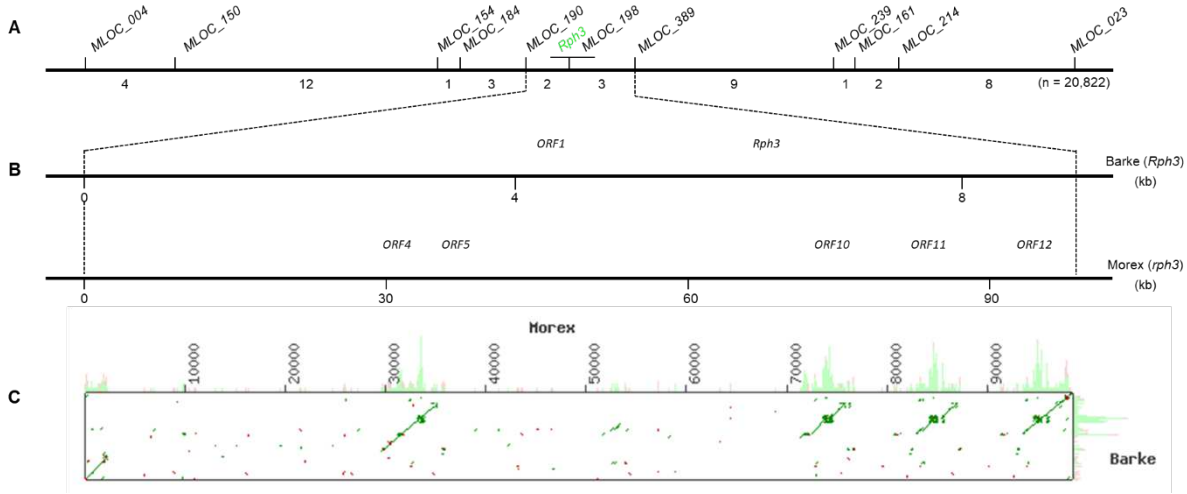

Fig. SI14. Genomic structures of the *Rph3* locus in resistant (Barke) and susceptible (Morex) cultivars. (*A*) Genetic map of the *Rph3* locus. (*B*) Physical maps of the *Rph3* locus in cvs. Barke (*Rph3*) and Morex (*rph3*). In cv. Barke, the *Rph3* locus was located in an 8,519-bp region containing putative genes named *ORF1* (black arrow) and *Rph3* (green arrow). In cv. Morex, the same flanked interval was 98,478 bp and contained 12 putative genes named *ORF1* to *ORF12,* among which *ORF4* (black arrow) was a homolog of *ORF1* in cv. Barke and four genes *ORF5*, *ORF10*, *ORF11*, and *ORF12* (green arrows) were homologs of *Rph3*. (*C*) Dot plot created using the DNA sequence of the *Rph3* locus in cvs. Barke and Morex. The second half of the 8.5-kb DNA fragment in cv. Barke was repeated four times in cv. Morex, where four homologs of *Rph3* were detected.

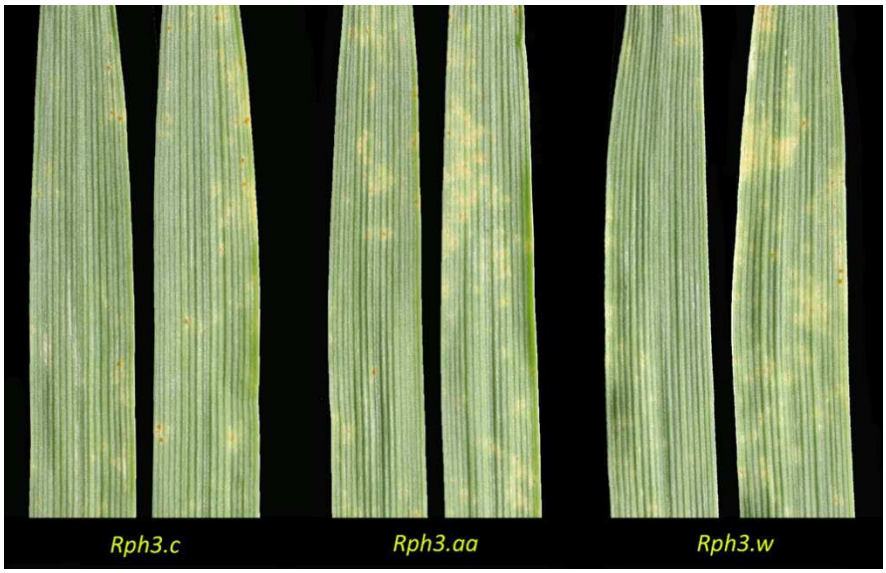

Fig. SI15. The responses of various postulated alleles of the *Rph3* gene to the *P. hordei* pathotype 5453 P+. In all three lines, 86ZBY99 carrying *Rph3.c*, 87ZBY99 carrying *Rph3.aa*, and 88ZBY99 carrying *Rph3.w*, the infection type was similar, with tiny colonies and occasional uredinia surrounded by chlorosis. All resistant parents in mapping populations (*SI Appendix*, Table S4) carry the *Rph3.c* allele.

TABLE TITLE

Table S1. The predominance of *P. hordei* pathotype virulent for the *Rph3* gene in Australia

Table S2. Marker genotype of recombinant inbred lines bred from the cross cvs. Tallon x Scarlett used for constructing the basic map of *Rph3*

Table S3. Pedigrees and gene postulation of the barley materials used in the construction of genetic map, mutant population, and the complementation test

Table S4. The mapping populations used for high-resolution mapping of the *Rph3* locus

Table S5. DNA markers used to construct the high-resolution map of the *Rph3* locus

Table S6. Marker genotype of critical homozygote recombinants in the vicinity of the resistance gene *Rph3* for constructing the high-resolution map

Table S7. Description of EMS induced mutants in the *Rph3* locus

Table S8. Barley induced mutants selected for *Rph3* using forward genetics

Table S9. Progeny test of *Rph3* transgenic plants in barley

Table S10. The differential expressed genes identified in BW746 challenged with *Rph3*-avirulent pathotype of *P. hordei* at two days post-inoculation

Table S11. PCR primers used for amplification and re-sequencing of 8.5kb, the *Rph3* locus in resistant haplotype

Table S12. The presence/absence of the *Rph3* gene in the barley core collection determined by molecular markers and multi-pathotype test

Table S13. GBS markers landing on the *Rph3* gene was used for detecting the gene in the worldwide barley collection

Table S14. The barley accession of IPK database carrying *Rph3* segment detected by GBS marker landing on the gene

Table S15. The Wild Barley Diversity Collection (WBDC) provided by University of Minnesota

Table S16. Virulence profile of *P. hordei* and *P. triticina* pathotypes used in this study

Table S17. Primers used for the expression analysis

Supplementary Files

This is a list of supplementary files associated with this preprint. Click to download.

- SupplementarytablesDingetal.xlsx